

BornAgain Developers Reference Physics and Numerics

Work in progress

Last updated May 31, 2023

edited by Joachim Wuttke

Scientific Computing Group
Jülich Centre for Neutron Science
at Heinz Maier-Leibnitz Zentrum Garching
Forschungszentrum Jülich GmbH

For information about BornAgain, see the reference paper Pospelov et al 2020 [1] and the web docs at <https://www.bornagainproject.org>.

This reference provides some of the theory behind the code. It is principally targetted at fellow developers.

Copyright: Forschungszentrum Jülich GmbH 2013–2023

License: Creative Commons CC-BY-SA

Editor: Joachim Wuttke

Authors: BornAgain developers, see git log
Scientific Computing Group
at Heinz Maier-Leibnitz Zentrum (MLZ) Garching

Disclaimer: Software and documentation are work in progress.
We cannot guarantee correctness and accuracy.
If in doubt, contact us for assistance or scientific collaboration.

Contents

1	Wave propagation and scattering	1:1
1.1	Wave propagation	1:1
1.1.1	Neutrons	1:1
1.1.2	Neutrons in a magnetic field	1:3
1.1.3	X-rays	1:3
1.1.4	Unified wave equation	1:5
1.2	Distorted-wave Born approximation	1:5
1.2.1	Distortion versus perturbation	1:6
1.2.2	Differential cross section	1:7
2	Flat multilayer systems	2:1
2.1	Wave propagation and scattering in layered samples	2:1
2.1.1	Wave propagation in 2+1 dimensions	2:1
2.1.2	The four DWBA terms	2:2
2.1.3	DWBA for layers with constant mean SLD	2:3
2.1.4	Modifications for X-rays	2:5
2.1.5	Wave amplitudes	2:6
2.2	Solution of the split boundary problem	2:8
2.2.1	The split boundary problem	2:9
2.2.2	Recursive solution	2:10
2.3	Implementation	2:10
2.3.1	Call chain	2:11
2.3.2	Scalar fluxes	2:12
2.4	Vanishing vertical wavenumber, evanescent case etc	2:13
3	Scattering by rough interfaces	3:1
3.1	Propagation through graded interfaces	3:1
3.1.1	Interface with tanh profile	3:1
3.1.2	Névot-Croce factor	3:3
3.2	Scattering by a rough interface	3:3
3.2.1	Scattering in DWBA	3:4
3.2.2	Random potential	3:5
3.2.3	Covariance ex machina	3:5
3.2.4	Sharp, rough interface	3:6
3.2.5	Stepwise reference potential	3:7

3.2.6	One-step reference potential	3:8
3.2.7	Gaussian roughness	3:9
3.2.8	Analytic plane waves approximation	3:10
3.2.9	Refracted waves, linearized correlation	3:11
3.2.10	Horizontal correlations	3:11
3.3	Literature review: reflectivity and scattering from rough surfaces . . .	3:12
4	Polarized wave propagation and scattering	4:1
4.1	Polarized neutrons	4:1
4.1.1	Wave equation and propagation within one layer	4:1
4.1.2	Wave propagation across layers	4:2
4.2	From old document “Reflectivity”	4:4
4.2.1	Transfer Matrix Method	4:4
4.2.2	Parratt Formalism	4:6
4.3	From old document “Stratified”	4:7
4.3.1	Wave equation and operator \mathbf{p}	4:7
4.3.2	Solution for stratified samples	4:8
4.3.3	Evaluation of the phase factors	4:9
4.3.4	The split boundary problem	4:9
4.4	From old document “PolarizedImplementation”	4:11
4.4.1	Transfer Matrix	4:11
4.4.2	Intensity Analysis	4:11
4.4.3	Numerically Stable Implementation	4:13
4.4.4	Evaluation of the Matrices $\underline{\underline{p}}$ and $\underline{\underline{p}}^{-1}$	4:15
4.4.5	Evaluation of the Phase Factors	4:16
4.4.6	Roughness	4:17
4.4.7	Reflection Matrix and Boundary Conditions	4:20
4.4.8	Amplitudes for DWBA Computations	4:20
4.4.9	Limiting Case $\kappa \rightarrow 0$	4:21
4.4.10	Test Suite	4:21
4.4.11	Magnetic Field in BornAgain	4:21
4.4.12	Further (Potential) Problems	4:22
5	Instrument simulation	5:1
5.1	Incoming beam and resolution	5:1
5.2	Detector images	5:1
5.2.1	Pixel coordinates, scattering angles, and \mathbf{q} components	5:2
5.2.2	Intensity transformation	5:5
	Bibliography	X:1
	List of Symbols	Y:1
	Index	Z:1

1 Wave propagation and scattering

{SSca}

This chapter introduces the formalism to described neutron and X-ray propagation and scattering, as needed for the analysis of grazing-incidence small-angle scattering (GISAS) experiments.

1.1 Wave propagation

{Swave}

In this section, we review the wave equations that describe the propagation of neutrons (Secs. 1.1.1 and 1.1.2) and X-rays (Sec. 1.1.3) in matter, and combine them into a unified wave equation (Sec. 1.1.4) that is the base for the all following analysis. This provides justification and background for Eqns. 1–3 in the BornAgain reference paper [1].

1.1.1 Neutrons

{SnScalar}

The scalar wavefunction $\psi(\mathbf{r}, t)$ of a free neutron in absence of a magnetic field is governed by the Schrödinger equation

$$i\hbar\partial_t\psi(\mathbf{r}, t) = \left\{ -\frac{\hbar^2}{2m}\nabla^2 + V(\mathbf{r}) \right\} \psi(\mathbf{r}, t). \quad (1.1) \quad \{\{\text{ESchrodi1}\}\}$$

Since BornAgain only aims at modelling elastic scattering, any time dependence of the potential is averaged out in the definition $V(\mathbf{r}) := \langle V(\mathbf{r}, t) \rangle$. Inelastic scattering, in principle, can be accounted for by an extra contribution damping.¹ Therefore we only need to consider monochromatic waves with given frequency ω . In consequence, the wavefunction

$$\psi(\mathbf{r}, t) = \psi(\mathbf{r})e^{-i\omega t} \quad (1.2) \quad \{\{\text{Estationarywave}\}\}$$

factorizes into a stationary wave and a time-dependent phase factor. In the following, we will characterize the incoming radiation not by its energy $\hbar\omega$, but by its *vacuum wavenumber* K , given by the dispersion relation

$$\hbar\omega = \frac{(\hbar K)^2}{2m}. \quad (1.3) \quad \{\{\text{Estationarywave}\}\}$$

¹This is not explicitly supported in the software, but users are free to increase the imaginary part of the refractive index to emulate damping by inelastic losses.

{Flosses}

The Schrödinger equation (1.1) then takes the simple form

$$\{\nabla^2 + K^2 - 4\pi v_{\text{nucl}}(\mathbf{r})\} \psi(\mathbf{r}) = 0 \quad (1.4)$$

with the rescaled form of Fermi's pseudopotential

$$v_{\text{nucl}}(\mathbf{r}) := \frac{m}{2\pi\hbar^2} V(\mathbf{r}) = \sum_j \langle b_j \delta(\mathbf{r} - \mathbf{r}_j(t)) \rangle. \quad (1.5)$$

The sum runs over all nuclei exposed to ψ . The subscript “nucl” designates nuclear as opposed to magnetic scattering. The *bound scattering length* b_j is isotope specific; values are tabulated [2].

In *small-angle scattering*, as elsewhere in *neutron optics* [3], the potential can be coarse-grained by spatially averaging over at least a few atomic diameters,

$$v_{\text{nucl}}(\mathbf{r}) = \sum_s b_s \rho_s(\mathbf{r}), \quad (1.6)$$

where the sum now runs over chemical elements, $b_s := \langle b_j \rangle_{j \in s}$ is the bound *coherent* scattering length, and ρ_s is a number density. In passing from (1.5) to (1.6), we neglected *Bragg scattering* from atomic-scale correlation, and *incoherent scattering* from spin or isotope related fluctuations of b_j . In small-angle experiments, these types of scattering only matter as loss channels.² Furthermore, incoherent scattering, as inelastic scattering, contributes to the diffuse background in the detector. In conclusion, the coarse-grained neutron optical potential (1.6) is just a *scattering length density* (SLD) [3, eq. 2.8.37].

In general, the incident neutron beam in a scattering experiment is not a *pure* quantum state, but a statistical mixture of such states, and must therefore be described by a density matrix,

$$\hat{\rho} := \sum_j p_j |\psi_j\rangle \langle \psi_j|, \quad (1.7)$$

where p_j is the probability of pure state ψ_j . Let us define the wave vector operator $\hat{\mathbf{k}}$ and the flux operator

$$\hat{\mathbf{J}} := |\mathbf{r}\rangle \langle \mathbf{r}| \hat{\mathbf{k}} + \hat{\mathbf{k}}^\dagger |\mathbf{r}\rangle \langle \mathbf{r}|. \quad (1.8)$$

The current density, or *flux*, is then given by

$$\mathbf{J}(\mathbf{r}) := \text{Tr}\{\hat{\rho}\hat{\mathbf{J}}\} \propto \sum_j p_j \left\{ \psi_j(\mathbf{r})^* \frac{\nabla}{2i} \psi_j(\mathbf{r}) - \psi_j(\mathbf{r}) \frac{\nabla}{2i} \psi_j(\mathbf{r})^* \right\}. \quad (1.9)$$

This is in arbitrary units, since we do not impose a specific normalization on the unbound wavefunction ψ . To compute scattering cross sections, we will only need the *ratio* of scattered to incident flux. Mostly we will assume pure states to be *plane waves*

$$\psi_{\mathbf{k}}(\mathbf{r}) := e^{i\mathbf{k}\mathbf{r}}. \quad (1.10)$$

²Same remark as in Footnote 1: To model these losses, use the imaginary part of the refractive index.

In vacuum, the wavevector \mathbf{k} purely real. We replace the sum in (1.7) by an integral, and find that the flux is simply

$$\mathbf{J}(\mathbf{r}) = \int d^3k p_{\mathbf{k}} |\psi_{\mathbf{k}}(\mathbf{r})|^2 \mathbf{k}. \quad (1.11)$$

1.1.2 Neutrons in a magnetic field

In presence of a magnetic field, the propagation of free neutrons becomes spin dependent. Therefore the scalar wavefunction of Sec. 1.1.1 must be replaced by spinor Ψ . The magnetic moment μ_n of the neutron couples to the magnetic induction \mathbf{B} [4, 5]. With the coupling term, the Schrödinger equation (1.1) becomes

$$\left\{ -\frac{\hbar^2}{2m} \nabla^2 + V(\mathbf{r}) + \mu_n \mathbf{B}(\mathbf{r}) \hat{\boldsymbol{\sigma}} - \hbar\omega \right\} \Psi(\mathbf{r}) = 0, \quad (1.12)$$

where $\hat{\boldsymbol{\sigma}}$ is the Pauli vector, composed of the three Pauli matrices. We introduce the reduced field

$$\mathbf{b} := \frac{m\mu_n}{2\pi\hbar^2} \mathbf{B}, \quad (1.13)$$

to rewrite the Schrödinger equation in analogy to (1.4) as

$$\left\{ \nabla^2 + K^2 - 4\pi v_{\text{nucl}}(\mathbf{r}) - 4\pi \mathbf{b}(\mathbf{r}) \hat{\boldsymbol{\sigma}} \right\} \Psi(\mathbf{r}) = 0. \quad (1.14)$$

The density matrix (1.7) becomes

$$\hat{\rho} := \sum_i p_i |\Psi_i\rangle \langle \Psi_i|. \quad (1.15)$$

The total flux is still given by (1.8) and (1.9). Beam polarization is described by an appropriate density matrix.

1.1.3 X-rays

The propagation of X-rays is governed by Maxwell's equations,

$$\nabla \times \mathbf{E} = -\partial_t \mathbf{B}, \quad \nabla \mathbf{B} = 0, \quad \mathbf{B} = \mu(\mathbf{r}) \mu_0 \mathbf{H}, \quad (1.16)$$

$$\nabla \times \mathbf{H} = +\partial_t \mathbf{D}, \quad \nabla \mathbf{D} = 0, \quad \mathbf{D} = \epsilon(\mathbf{r}) \epsilon_0 \mathbf{E}.$$

Since BornAgain only addresses elastic scattering, we assume the permeability and permittivity tensors μ and ϵ to be time-independent. Therefore, as in Sec. 1.1.1, we only need to consider monochromatic waves with given frequency ω , and each of the fields \mathbf{E} , \mathbf{D} , \mathbf{H} , \mathbf{B} factorizes into a stationary field and a time-dependent phase factor.³ We will formulate the following in terms of the electric field

$$\mathbf{E}(\mathbf{r}, t) = \mathbf{E}(\mathbf{r}) e^{-i\omega t}. \quad (1.17)$$

³This phase factor can be defined with a plus or a minus sign in the exponent. Most texts on X-ray crystallography, including influential texts on GISAXS [6], prefer the *crystallographic convention* with a plus sign. In BornAgain, we prefer the opposite *quantum-mechanical convention* for consistency with the neutron case (1.2), where the minus sign is an inevitable consequence of the standard form of the Schrödinger equation.

The other three fields can be obtained from \mathbf{E} by straightforward application of (1.16).

Since magnetic refraction or scattering is beyond the scope of BornAgain, the relative magnetic permeability tensor is always $\mu(\mathbf{r}) = 1$. As customary in SAXS and GISAXS, we assume that the dielectric properties of the material are those of a polarizable electron cloud.⁴ Thereby the relative dielectric permittivity tensor ϵ becomes a scalar,

$$\epsilon(\mathbf{r}) = 1 - \frac{4\pi r_e}{K^2} \rho(\mathbf{r}), \quad (1.18) \quad \{\text{EstationaryX}\}$$

with the classical electron radius $r_e = e^2/mc^2 \simeq 2.8 \cdot 10^{-15}$ m, the electron number density $\rho(\mathbf{r})$, and the vacuum wavenumber K , given by the dispersion relation

$$K^2 = \mu_0 \epsilon_0 \omega^2. \quad (1.19)$$

With these simplifying assumptions about ϵ and μ , Maxwell's equations yield the wave equation

$$\nabla \times \nabla \times \mathbf{E} = K^2 \epsilon(\mathbf{r}) \mathbf{E}. \quad (1.20) \quad \{\{\text{ENabCrossNabE}\}\}$$

Using a standard identity from vector analysis, it can be brought into the more tractable form

$$\{\nabla^2 - \nabla \cdot \nabla + K^2 \epsilon(\mathbf{r})\} \mathbf{E}(\mathbf{r}) = 0. \quad (1.21) \quad \{\{\text{ENabNabE}\}\}$$

It is well known that the electromagnetic energy flux is given by the Poynting vector. However, its standard definition, $\mathbf{S} := \mathbf{E} \times \mathbf{H}$, is not applicable here because it only holds for *real* fields. With our complex notation, it must be replaced by

$$\mathbf{S} := \text{Re } \mathbf{E}(\mathbf{r}, t) \times \text{Re } \mathbf{H}(\mathbf{r}, t). \quad (1.22) \quad \{\text{ENabNabE}\}$$

For stationary oscillations (1.17), the time average is

$$\langle \mathbf{S} \rangle = \frac{1}{4} \langle \mathbf{E}(\mathbf{r}) \times \mathbf{H}(\mathbf{r})^* + \text{c. c.} \rangle. \quad (1.23)$$

We specialize to vacuum with $\epsilon(\mathbf{r}) = 1$, and obtain

$$\langle \mathbf{S} \rangle = \frac{1}{4i\omega\mu_0} (\mathbf{E}^*(\mathbf{r}) \times (\nabla \times \mathbf{E}(\mathbf{r})) + \text{c. c.}). \quad (1.24)$$

For a plane wave $\mathbf{E}(\mathbf{r}) = \mathbf{E}_{\mathbf{k}} e^{i\mathbf{k}\mathbf{r}}$, we find

$$\langle \mathbf{S} \rangle = \frac{1}{2\omega\mu_0} |\mathbf{E}_{\mathbf{k}}|^2 \text{Re } \mathbf{k}, \quad (1.25)$$

which confirms the common knowledge that the radiation intensity counted in a detector is proportional to the squared electric field amplitude.

⁴This is occasionally called the *Laue model* [7].

1.1.4 Unified wave equation

As in Eqns. 1–3 of Ref. [1], we combine all the above in a unified wave equation

{SuniWave}

$$(D_0 - 4\pi\hat{v}(\mathbf{r})) \Psi(\mathbf{r}) = 0 \quad (1.26) \quad \{\{\text{EWAVE}\}\}$$

with the vacuum wave operator

$$D_0 := \begin{cases} \nabla^2 + K^2 & \text{for neutrons,} \\ \nabla^2 - \nabla \cdot \nabla + K^2 & \text{for X-rays} \end{cases} \quad (1.27) \quad \{\{\text{EDo}\}\}$$

and the potential⁵

$$\hat{v}(\mathbf{r}) := \begin{cases} v_{\text{nucl}}(\mathbf{r}) & \text{for neutrons (scalar),} \\ v_{\text{nucl}}(\mathbf{r}) + \mathbf{b}(\mathbf{r})\hat{\sigma} & \text{for neutrons (spinorial),} \\ K^2(1 - \epsilon(\mathbf{r}))/4\pi & \text{for X-rays.} \end{cases} \quad (1.28) \quad \{\{\text{ETV}\}\}$$

The generic wave amplitude Ψ shall represent the scalar neutron wavefunction ψ , the spinor Ψ , or the electric field \mathbf{E} , as applicable. The hat in \hat{v} denotes an operator in spin space; it can be ignored in the scalar cases.

⁵This corrects Eq. 3 in our reference paper [1], which had a sign error in the X-ray case.

{SDWBA}

{Sdecompose}

{{Edecompose}}

{{EDPsi}}

{EDPsi}

{{EDPsi0}}

{{EnkK}}

1.2 Distorted-wave Born approximation

Neutron or X-ray scattering by condensed matter is usually described in *Born approximation* (BA), which treats the potential $\hat{v}(\mathbf{r})$ as a small perturbation. This is not adequate if incident or scattered wave propagate under small grazing angles, as refraction and reflection are no longer small. For grazing-incidence small-angle scattering, we need the more generic *distorted-wave Born approximation* (DWBA).⁶

1.2.1 Distortion versus perturbation

To get started, we decompose the potential (1.28) into a more *regular* and a more *fluctuating* part:

$$\hat{v}(\mathbf{r}) =: \bar{v}(\mathbf{r}) + \delta\hat{v}(\mathbf{r}). \quad (1.29)$$

The *distortion field* \bar{v} comprises regular, well-known features of the sample. The *perturbation potential* $\delta\hat{v}$ stands for the more irregular, unknown features of the sample one ultimately wants to study in a scattering experiment. The wave equation (1.26) shall henceforth be written as

$$D(\mathbf{r})\Psi(\mathbf{r}) = 4\pi\delta\hat{v}(\mathbf{r}) \quad (1.30)$$

with the *distorted wave operator*

$$D(\mathbf{r}) := D_0 - 4\pi\bar{v}(\mathbf{r}). \quad (1.31)$$

Only $\delta\hat{v}$ shall be treated as a perturbation. The propagation of incident and scattered waves under the influence of \bar{v} , in contrast, shall be handled exactly, through analytical solution of the *unperturbed distorted wave equation*

$$D(\mathbf{r})\Psi(\mathbf{r}) = 0. \quad (1.32)$$

The solutions are called *distorted* because they differ from the plane waves obtained in the vacuum case $\bar{v} = 0$.

Except for neutrons in a magnetic field the distortion field is scalar so that it can be expressed through the *refractive index*

$$n(\mathbf{r}) := \sqrt{1 - \frac{4\pi\bar{v}(\mathbf{r})}{K^2}} = \begin{cases} \sqrt{1 - 4\pi\bar{v}(\mathbf{r})/K^2} & \text{for neutrons,} \\ \sqrt{\epsilon(\mathbf{r})} & \text{for X-rays.} \end{cases} \quad (1.33)$$

⁶The DWBA was originally devised by Massey and Mott (ca 1933) for collisions of charged particles. Summaries can be found in some quantum mechanics textbooks (Messiah, Schiff) and in monographs on scattering theory (e. g. Newton). The first explicit applications to grazing-incidence scattering were published in 1982: Vineyard [8] discussed X-ray scattering, but failed to account for the distortion of the scattered wave; Mazur and Mills [9] deployed heavy formalism to compute the inelastic neutron scattering cross section of ferromagnetic surface spin waves from scratch. A concise derivation of the DWBA cross section was provided by Dietrich and Wagner (1984/85) for X-rays [10] and neutrons [11]. Unfortunately, their work was overlooked in much of the later literature, which often fell back to less convincing derivations.

If $\bar{v}(\mathbf{r})$ or $\epsilon(\mathbf{r})$ has an imaginary part, describing absorption, then $n(\mathbf{r})$ is a complex number. Conventionally, n is parameterized by two real numbers:

$$n =: 1 - \delta + i\beta. \quad (1.34) \quad \{\{\text{Endb1}\}\}$$

For thermal neutrons and X-rays, δ and β are almost always nonnegative,⁷ and much smaller than 1. This explains why in most scattering geometries the ordinary Born approximation with $\bar{v} \equiv 0$ is perfectly adequate. In layered samples under grazing incidence, however, even small differences in n can cause substantial *refraction* and *reflection*. To model GISAS, therefore, it is necessary to use DWBA, and to let \bar{v} represent the average vertical refractive index profile $\bar{n}(z)$.

1.2.2 Differential cross section

\{\{\text{SdiffCross}\}\}

The ratio of the scattered flux hitting an infinitesimal detector area $r^2 d\Omega$ to the incident flux is expressed as a *differential cross section*

$$\frac{d\sigma}{d\Omega} := \frac{r^2 J(\mathbf{r})}{J_i}. \quad (1.35) \quad \{\{\text{Exsectiondef}\}\}$$

The geometric factors that are needed to convert $d\sigma/d\Omega$ into detector counts will be discussed below in Sec. 5.2.

From standard textbooks we take the generic differential cross section of elastic scattering in first order Born approximation,⁸

$$\frac{d\sigma}{d\Omega} = |\langle \psi_i | \delta \hat{v} | \psi_f \rangle|^2, \quad (1.36) \quad \{\{\text{Exsection}\}\}$$

where the matrix element in Dirac bra-ket notation stands for the integral

$$\langle \psi_i | \delta \hat{v} | \psi_f \rangle := \int d^3r \psi_i^*(\mathbf{r}) \delta \hat{v}(\mathbf{r}) \psi_f(\mathbf{r}). \quad (1.37) \quad \{\{\text{Etrama}\}\}$$

For brevity and mathematical convenience, the integral has no bounds and therefore formally runs over the entire space. However, $\delta \hat{v}(\mathbf{r})$ is nonzero only if \mathbf{r} lies inside the finite sample volume.

In ordinary (non-distorted) Born approximation, the incident wavefunction ψ_i is a plane wave (1.10). By means of a far-field expansion, the outgoing spherical wave ψ_f , traced back from the detector towards the sample, is also approximated as a plane wave. Thereby (1.37) becomes a Fourier integral

$$\langle \psi_i | \delta \hat{v} | \psi_f \rangle = \int d^3r e^{-i\mathbf{k}_i \mathbf{r}} \delta \hat{v}(\mathbf{r}) e^{i\mathbf{k}_f \mathbf{r}} = \int d^3r e^{i\mathbf{q} \mathbf{r}} \delta \hat{v}(\mathbf{r}) \quad (1.38) \quad \{\{\text{Etramaq}\}\}$$

with the scattering vector

$$\mathbf{q} := \mathbf{k}_f - \mathbf{k}_i. \quad (1.39) \quad \{\{\text{Etramaq}\}\}$$

⁷The plus sign in front of $i\beta$ is a consequence of the quantum-mechanical sign convention; in the X-ray crystallography convention it would be a minus sign.

⁸For a particularly detailed derivation see Schober's lecture notes on neutron scattering [12].

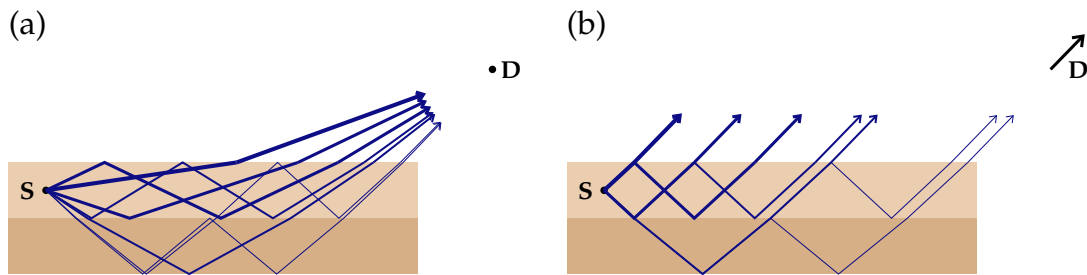


Figure 1.1: (a) In a multilayer sample, the scattered wave propagates from the scattering center S towards the detector D through different paths, due to partial reflection by interfaces. (b) In far-field approximation, the detector location is so remote that all rays leaving the sample can be considered parallel. In consequence, when the scattered wave is traced back from the detector it can be considered plane until it reaches the sample.

{Fgreen1}

This plane-wave approximation breaks down under grazing incidence as refraction and reflection by surfaces and interfaces cannot be neglected. While (1.36) still holds, (1.37) does not. In DWBA, the incident wave ψ_i ceases to be plane when it reaches the sample (Fig. 1.1). Inside the sample it evolves according to the unperturbed wave equation (1.32). Similarly, the scattered wave ψ_f , traced back from the detector and in first order of far-field expansion, is a plane wave outside the sample, and must be traced back inside the sample according to (1.32). The wave propagation inside a discrete multilayer sample will be worked out in Chapter 2.

2 Flat multilayer systems

{sec:Multilayers}

This chapter specializes the DWBA for a multilayer system with $\bar{v}(\mathbf{r}) = \bar{v}(z)$.

2.1 Wave propagation and scattering in layered samples

{Swave21}

2.1.1 Wave propagation in 2+1 dimensions

{Sgrazingwave}

We now specialize the results from Chapter 1 to wave propagation in a sample that is, on average, translationally invariant in 2 dimensions. Following standard convention, we choose the surface of the sample in the xy plane, and its normal along z . In visualizations, we will always represent the xy plane as *horizontal*, and the z axis as upward *vertical*, although there are “horizontal” reflectometers where the sample is upright to allow for a horizontal scattering plane.

Scattering from such systems will be studied in distorted-wave Born approximation. To determine the neutron scattering cross section (1.36), we need to determine the incident and final wavefunctions ψ_i and ψ_f . Vertical variations of the refractive index $n(z)$ cause refraction and reflection. For waves propagating at small glancing angles, the reflectance can take any value between 0 and 1, even though $1 - n$ is only of the order 10^{-5} or smaller. Such zeroth-order effects cannot be accounted for by perturbative scattering theory. Instead, we need to deal with refraction and reflection from the onset, in the wave propagation equation. Accordingly, the SLD decomposition (1.29) takes the form

$$v(\mathbf{r}) = \bar{v}(z) + \delta v(\mathbf{r}), \quad (2.1) \quad \{\{Edecompose_z\}\}$$

and the unperturbed distorted wave equation (1.32) becomes

$$\{\nabla^2 + k(z)^2\} \psi(\mathbf{r}) = 0. \quad (2.2) \quad \{\{EWaveZ\}\}$$

Below and above the sample, $k(z) = \text{const}$: in these regions, $\psi(\mathbf{r})$ is a superposition of plane waves. The exciting wavefunction is

$$\psi_e(\mathbf{r}) = e^{i\mathbf{k}_{\parallel}\mathbf{r}_{\parallel} + ik_{\perp}z}, \quad (2.3) \quad \{\{Epsiminus\}\}$$

The subscripts \parallel and \perp refer to the sample xy plane. The wavevector components \mathbf{k}_{\parallel} and k_{\perp} must fulfill

$$k(z)^2 = \mathbf{k}_{\parallel}^2 + k_{\perp}^2. \quad (2.4) \quad \{\{Epsiminus\}\}$$

Continuity across the sample implies

$$\mathbf{k}_{\parallel} = \text{const.} \quad (2.5) \quad \{\{\text{Ekconst}\}\}$$

From here on, we abbreviate

$$\kappa := k_{\perp}. \quad (2.6) \quad \{\{\text{Ekconst}\}\}$$

When the incident wave hits the sample, it is wholly or partly reflected. Therefore, the full the solution of (2.2) in the half space of the radiation source is

$$\psi(\mathbf{r}) = e^{i\mathbf{k}_{\parallel}\mathbf{r}_{\parallel} + i\kappa_e z} + R e^{i\mathbf{k}_{\parallel}\mathbf{r}_{\parallel} - i\kappa_e z} \quad (2.7) \quad \{\{\text{Eref1}\}\}$$

with a complex reflection coefficient R . The reflected flux is given by the reflectance $|R|^2$. In the opposite halfspace, the solution of (2.2) is simply

$$\psi(\mathbf{r}) = T e^{i\mathbf{k}_{\parallel}\mathbf{r}_{\parallel} + i\kappa_e z} \quad (2.8) \quad \{\{\text{Etra1}\}\}$$

with a complex transmission coefficient T . The transmitted flux is given by the transmittance $|T|^2$. As before, subscript e stands for the exciting wave in vacuum outside the sample.

Within the sample, the wave equation (2.2) is solved by the factorization ansatz

$$\psi(\mathbf{r}) = e^{i\mathbf{k}_{\parallel}\mathbf{r}_{\parallel}} \phi(z). \quad (2.9) \quad \{\{\text{Ekpar}\}\}$$

The vertical wavefunction $\phi(z)$ is governed by the one-dimensional wave equation

$$\left\{ \partial_z^2 + k(z)^2 - k_{\parallel}^2 \right\} \phi(z) = 0. \quad (2.10) \quad \{\{\text{Ewavez}\}\}$$

As solution of a differential equation of second degree, $\phi(z)$ can be written as superposition of a downward travelling wave $\phi^-(z)$ and an upward travelling wave $\phi^+(z)$. Accordingly, the three-dimensional wavefunction can be written as

$$\psi(\mathbf{r}) = \psi^-(\mathbf{r}) + \psi^+(\mathbf{r}). \quad (2.11) \quad \{\{\text{Epsisumpm}\}\}$$

2.1.2 The four DWBA terms

All the above holds not only for the incident wavefunction ψ_i , but also for the wavefunction ψ_f that is tracked back from a detector pixel towards the sample. Therefore the scattering matrix element involves two incident and two final partial wavefunctions. The resulting sum

$$\langle \psi_i | \delta v | \psi_f \rangle = \langle \psi_i^- | \delta v | \psi_f^- \rangle + \langle \psi_i^- | \delta v | \psi_f^+ \rangle + \langle \psi_i^+ | \delta v | \psi_f^- \rangle + \langle \psi_i^+ | \delta v | \psi_f^+ \rangle \quad (2.12) \quad \{\{\text{Edwba4}\}\}$$

is depicted in Figure 2.1. It can be written in an obvious shorthand notation

$$\langle \psi_i | \delta v | \psi_f \rangle = \sum_{\pm_i} \sum_{\pm_f} \langle \psi_i^{\pm} | \delta v | \psi_f^{\pm} \rangle. \quad (2.13) \quad \{\{\text{Edwba}\}\}$$

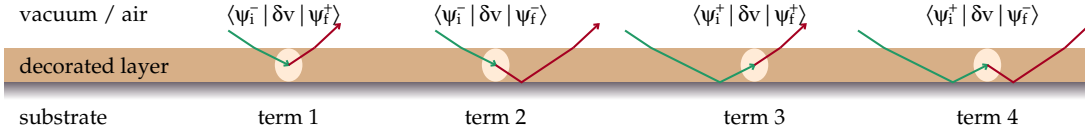


Figure 2.1: The four terms in the DWBA scattering matrix element (2.13). Note that this is a highly simplified visualization. In particular, it does not show multiple reflections of incoming or scattered radiation, though they are properly accounted for by DWBA theory and by all simulation software.

{Fdwba4terms}

This equation contains the essence of the DWBA for GISAS, and is the base for all scattering models implemented in BornAgain. Since $\langle \psi_i | \delta v | \psi_f \rangle$ appears as a squared modulus in the differential cross section (1.36), the four terms of (2.13) can interfere with each other, which adds to the complexity of GISAS patterns.

BornAgain supports multilayer samples with refractive index discontinuities at layer interfaces. Conventions for layer numbers and interface coordinates are introduced in Figure 2.2. A sample has N layers, including the semi-infinite bottom and top layers. Numbering is from top to bottom, and from 0 to $N - 1$ as imposed by the programming languages C++ and Python. Each layer l has a constant refractive index n_l and a constant wavenumber $k_l := K_{\text{vac}} n_l$. Any up- or downward travelling solution of the wave equation shall be written as a sum over partial wavefunctions,

$$\psi^\pm(\mathbf{r}) = \sum_l \psi_l^\pm(\mathbf{r}), \quad (2.14) \quad \{\{\text{Epsipmsuml}\}\}$$

with the requirement

$$\psi_l^\pm(\mathbf{r}) = 0 \text{ for } \mathbf{r} \text{ outside layer } l. \quad (2.15) \quad \{\{\text{Epsipmloutside}\}\}$$

The DWBA matrix element (2.13) then takes the form

$$\langle \psi_i | \delta v | \psi_f \rangle = \sum_l \sum_{\pm_i} \sum_{\pm_f} \langle \psi_{i,l}^\pm | \delta v | \psi_{f,l}^\pm \rangle. \quad (2.16) \quad \{\{\text{Edwbal}\}\}$$

2.1.3 DWBA for layers with constant mean SLD

{SStep}

We now specialize to the case that $\bar{v}(z)$ is a step function: within each layer, $\bar{v}(z) =: v_l$ is constant. Accordingly, within the layer, the directional neutron wavefunction ψ_l^\pm is a plane wave and factorizes as in (2.9). Its amplitude A_l^\pm is determined recursively by Fresnel's transmission and reflection coefficients that are based on continuity conditions at the layer interfaces. This will be elaborated in Section 2.1.5. The vertical wavenumber is determined by (2.3) and (2.5),

$$\kappa_l^\pm = \pm \sqrt{k_l^2 - k_\parallel^2}. \quad (2.17) \quad \{\{\text{Ekperp1}\}\}$$

In the absence of absorption and above the critical angle, wavevectors are real so that we can describe the beam in terms of a glancing angle

$$\alpha_l := \arctan(\kappa_l / k_\parallel). \quad (2.18) \quad \{\{\text{Edef_alpha}\}\}$$

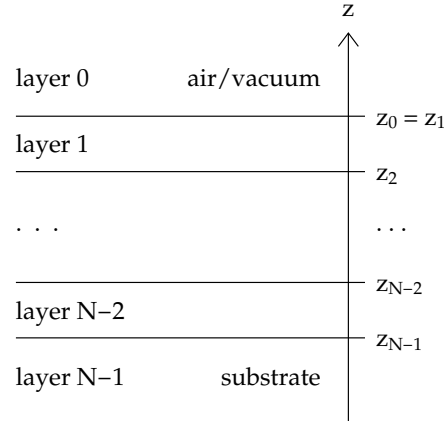


Figure 2.2: Conventions for layer numbers and interface coordinates. A sample has N layers, including the semi-infinite bottom and top layers. Layers are numbered from top to bottom. The top vacuum (or air) layer (which extends to $z \rightarrow +\infty$) has number 0, the substrate (extending to $z \rightarrow -\infty$) is layer $N - 1$. The parameter z_l is the z coordinate of the *top* interface of layer l , except for z_0 which is the coordinate of the *bottom* interface of the air or vacuum layer 0.

{Fdefz}

Equivalently,

$$k_{\parallel} = K n_l \cos \alpha_l. \quad (2.19) \quad \{\{Ekplllncos\}\}$$

Since k_{\parallel} is constant across layers, we have

$$n_l \cos \alpha_l = \text{the same for all } l, \quad (2.20) \quad \{\{ESnell\}\}$$

which is Snell's refraction law. In general, however, the vertical wavenumber κ_l , determined by k_l and k_{\parallel} as per (2.3), can become imaginary (total reflection conditions) or complex (absorbing layer). In these cases, glancing angles are no longer well defined, and the geometric interpretation of $\psi_l(\mathbf{r})$ less obvious. so that one has to fully rely on the algebraic formalism.

With the indicator function

$$\chi_l(\mathbf{r}) := \begin{cases} 1 & \text{if } z_l \leq z \leq z_{l+1}, \\ 0 & \text{otherwise,} \end{cases} \quad (2.21) \quad \{\{Echildef\}\}$$

the vertical wavefunction can be written

$$\phi_l^{\pm}(z) = A_l^{\pm} e^{\pm i \kappa_l (z - z_l)} \chi_l(z). \quad (2.22) \quad \{\{Ephizwj\}\}$$

The offset z_l has been included in the phase factor for later convenience. See ?? for the case of vanishing κ .

The DWBA transition matrix element (2.13) is

$$\langle \psi_i | \delta v | \psi_f \rangle = \sum_l \sum_{\pm_i} \sum_{\pm_f} A_{il}^{\pm_i*} A_{fl}^{\pm_f} \delta v_l(\mathbf{k}_{fl}^{\pm_f} - \mathbf{k}_{il}^{\pm_i}) \quad (2.23) \quad \{\{Edwba_m10\}\}$$

with the Fourier transform of the SLD restricted to layer l

$$\delta v_l(\mathbf{q}) := \int_{z_l}^{z_{l+1}} dz \int d^2 r_{\parallel} e^{i\mathbf{q}\mathbf{r}} \delta v(\mathbf{r}) = \int d^3 r e^{i\mathbf{q}\mathbf{r}} \delta v(\mathbf{r}) \chi_l(z). \quad (2.24) \quad \{\{\text{Echi j}\}\}$$

To alleviate later calculations, we number the four DWBA terms from 1 to 4 as shown in Fig. 2.1, and define the corresponding wavenumbers and amplitude factors and as

$$\begin{aligned} \mathbf{q}^1 &:= \mathbf{k}_f^+ - \mathbf{k}_i^-, & C^1 &:= A_i^{-*} A_f^+, \\ \mathbf{q}^2 &:= \mathbf{k}_f^- - \mathbf{k}_i^-, & C^2 &:= A_i^{-*} A_f^-, \\ \mathbf{q}^3 &:= \mathbf{k}_f^+ - \mathbf{k}_i^+, & C^3 &:= A_i^{+*} A_f^+, \\ \mathbf{q}^4 &:= \mathbf{k}_f^- - \mathbf{k}_i^+, & C^4 &:= A_i^{+*} A_f^-. \end{aligned} \quad (2.25) \quad \{\{\text{Eundef}\}\}$$

Accordingly, we can write (2.23) as

$$\langle \psi_i | \delta v | \psi_f \rangle = \sum_l \sum_u C_l^u \delta v_l(\mathbf{q}_l^u). \quad (2.26) \quad \{\{\text{Edwba_ml}\}\}$$

Since $\mathbf{k}_{\parallel} = \text{const}$, all wavevectors \mathbf{q}_l^u have the same horizontal component \mathbf{q}_{\parallel} ; they differ only in their vertical component $q_{l\perp}^u$.

2.1.4 Modifications for X-rays

\{\{\text{SmulayX}\}\}

We shall now translate the above results from unpolarized neutrons to X-rays. The vectorial amplitude of the electromagnetic field will require nontrivial modifications. In place of the factorization (2.9), we write

$$\mathbf{E}(\mathbf{r}) = e^{i\mathbf{k}_{\parallel}\mathbf{r}} \Phi(z). \quad (2.27) \quad \{\{\text{Edwba_ml}\}\}$$

In place of (2.22), the vertical wavefunction is

$$\Phi_l^{\pm}(z) = \mathbf{A}_l^{\pm} e^{\pm i\kappa(z-z_l)} \chi_l(z). \quad (2.28)$$

The vectorial character of \mathbf{A}_{wl}^{\pm} will require changes in Sec. 2.1.5. For electromagnetic radiation in nonmagnetic media, the boundary conditions at an interface with normal \mathbf{n} are [13, eq. 7.37]

$$\sum_{\pm} \bar{\epsilon} \mathbf{E}^{\pm} \mathbf{n} = \text{const}, \quad (2.29) \quad \{\{\text{Eb cE1}\}\}$$

$$\sum_{\pm} \mathbf{E}^{\pm} \times \mathbf{n} = \text{const}, \quad (2.30) \quad \{\{\text{Eb cE2}\}\}$$

$$\sum_{\pm} \mathbf{k}_l^{\pm} \times \mathbf{E}^{\pm} = \text{const}. \quad (2.31) \quad \{\{\text{Eb cE3}\}\}$$

We will only consider the two polarization directions, conventionally designated as p and s , defined in Figure 2.3. As some algebra on (2.29) to (2.31) would show, these are *principal axes*, meaning that if both incoming fields \mathbf{E}_{l-1}^- and \mathbf{E}_l^+ are strictly polarized

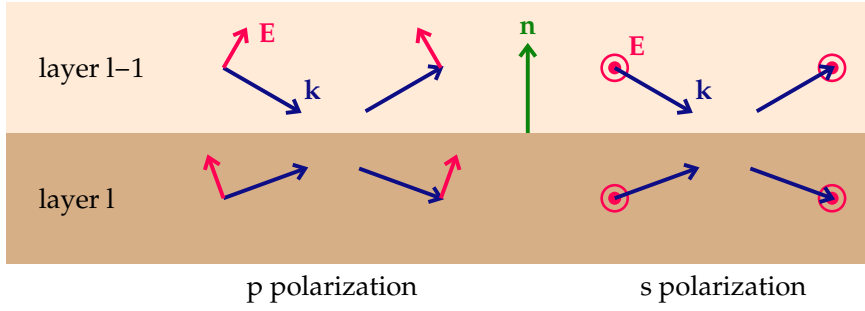


Figure 2.3: Conventions for polarization directions relative to a refracting interface: For p polarization, the electric field vector \mathbf{E} is parallel to the interface normal \mathbf{n} ; for s polarization, it is perpendicular (*senkrecht* in German). In either case, \mathbf{E} is perpendicular to the wavevector \mathbf{k} .

{Fspol1}

in either p or s direction, then the outgoing fields \mathbf{E}_{l-1}^+ and \mathbf{E}_l^- are polarized in the same direction. Conversely, if the incoming fields are mixtures of p and s polarization, then the outgoing fields will be, in general, mixed differently. Therefore if polarization factors are quantitatively important in an experiment, one should strive to accurately polarize the incident beam in p or s direction in order to avoid the extra complication of variably mixed polarizations.

Further algebra on (2.29) to (2.31) replicates the reflection law that relates \mathbf{k}^- and \mathbf{k}^+ and Snell's law (2.20). Taking these for granted, we only retain equations that are needed to determine the field amplitudes E^\pm . For p polarization they yield

$$\begin{pmatrix} k & k \\ -\kappa/k & \kappa/k \end{pmatrix} \begin{pmatrix} E^- \\ E^+ \end{pmatrix} = \text{const}, \quad (2.32)$$

{EbcE3}

and for s polarization

$$\begin{pmatrix} 1 & 1 \\ -\kappa & \kappa \end{pmatrix} \begin{pmatrix} E^- \\ E^+ \end{pmatrix} = \text{const}. \quad (2.33)$$

The latter equation can be brought into the form (2.38). In consequence, s -polarized X-rays are refracted and reflected in exactly the same ways as unpolarized neutrons.

For p polarization, ... (TODO)

2.1.5 Wave amplitudes

{Sacrolay}

The plane-wave amplitudes A_{wl}^\pm need to be computed recursively from layer to layer. Since these computations are identical for incident and final waves, we omit the subscript w in the remainder of this section. At layer interfaces, the optical potential changes discontinuously. From elementary quantum mechanics we know that piecewise solutions of the Schrödinger equations must be connected such that the wavefunction $\phi(\mathbf{r})$ and its first derivative $\nabla\phi(\mathbf{r})$ evolve continuously.

To deal with the coordinate offsets introduced in (2.22), we introduce the function

$$d_l := z_l - z_{l+1}, \quad (2.34)$$

{{Edldef}}

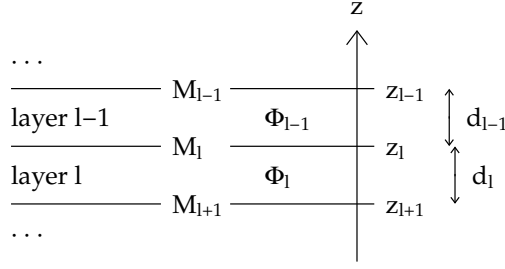


Figure 2.4: The transfer matrix M_l connects the wavefunctions Φ_l, Φ_{l-1} in adjacent layers. {Fboundary}

which is the thickness of layer l , except for $l = 0$, where the special definition of z_0 (Fig. 2.2) implies $d_0 = 0$. We consider the interface between layers l and $l - 1$, with $l = 1, \dots, N - 1$, as shown in Fig. 2.4. This interface has the vertical coordinate $z_l = z_{l-1} - d_{l-1}$. Accordingly, the continuity conditions at the interface are

$$\begin{aligned} \phi_l(z_l) &= \phi_{l-1}(z_{l-1} - d_{l-1}), \\ \partial_z \phi_l(z_l) &= \partial_z \phi_{l-1}(z_{l-1} - d_{l-1}). \end{aligned} \quad (2.35) \quad \{\{Econtcond\}\}$$

We abbreviate

$$\delta_l := e^{i\kappa_l d_l}. \quad (2.36) \quad \{\{Ddel1\}\}$$

Here and in the following, we will write the downward travelling transmitted and of the upward travelling reflected amplitude as

$$t_l := A_l^- \quad \text{and} \quad r_l := A_l^+. \quad (2.37) \quad \{\{Ddel1\}\}$$

For the plane waves (2.22), the continuity conditions (2.35) take the form

$$\begin{aligned} t_l + r_l &= t_{l-1} \delta_{l-1} + r_{l-1} \delta_{l-1}^{-1}, \\ -t_l \kappa_l + r_l \kappa_l &= -t_{l-1} \delta_{l-1} \kappa_{l-1} + r_{l-1} \delta_{l-1}^{-1} \kappa_{l-1}. \end{aligned} \quad (2.38) \quad \{\{Econt2\}\}$$

After some lines of linear algebra, we can rewrite this equation system as

$$\begin{pmatrix} t_{l-1} \\ r_{l-1} \end{pmatrix} = M_l \begin{pmatrix} t_l \\ r_l \end{pmatrix} \quad (2.39) \quad \{\{EcMc\}\}$$

with the transfer matrix¹

$$M_l := \Delta_{l-1} S_l, \quad (2.40) \quad \{\{EMi1\}\}$$

which we write using the phase rotation matrix

$$\Delta_l := \begin{pmatrix} \delta_l^{-1} & 0 \\ 0 & \delta_l \end{pmatrix} \quad (2.41) \quad \{\{DmatD\}\}$$

¹This approach is generally attributed to Abelès, who elaborated it in his thesis from 1949, published 1950. The usually cited paper [14] is no more than a short advertisement.

and the refraction matrix

$$S_l := \frac{1}{2} \begin{pmatrix} s_l^+ & s_l^- \\ s_l^- & s_l^+ \end{pmatrix} \tag{2.42} \quad \text{\texttt{\{DmatS\}}}$$

with coefficients

$$s_l^\pm := 1 \pm \kappa_l / \kappa_{l-1}. \tag{2.43} \quad \text{\texttt{\{Ds1pm\}}}$$

Energy conservation can be easily verified for real-valued wave numbers. The vertical flux is $J = |\Phi|^2 \kappa$. Under the action of either Δ or S ,

$$\kappa_l (|t_l|^2 - |r_l|^2) = \text{const for all } l. \tag{2.44} \quad \text{\texttt{\{EConservation\}}}$$

2.2 Solution of the split boundary problem

{Ssolvsplit}

2.2.1 The split boundary problem

{Ssplibou}

We now consider beam propagation through the entire multilayer sample, from the semiinfinite top layer at $l = 0$ to the semiinfinite substrate at $l = N - 1$, which for brevity shall be denoted by $\nu := N - 1$.

Let us assume that the radiation source or sink is located at $z > 0$. Then in the top layer, $t_0 = 1$ is given by the incident or back-traced final plane wave. In the substrate, $t_\nu = 0$ because there is no radiation coming from $z \rightarrow -\infty$. This leaves us with two unknown amplitudes, the overall coefficients of transmission t_ν and reflection r_0 . These two unknowns are connected by a system of two linear equations,

$$\begin{pmatrix} 1 \\ r_0 \end{pmatrix} = M \begin{pmatrix} t_\nu \\ 0 \end{pmatrix} \quad (2.45) \quad \{\{E1Ap\}\}$$

with the matrix product

$$M := M_1 \cdots M_\nu =: \begin{pmatrix} M_{tt} & M_{tr} \\ M_{rt} & M_{rr} \end{pmatrix}. \quad (2.46) \quad \{\{DM22\}\}$$

To apply this and all the following to the scattered beam in transmission GISAS (sink location $z < 0$), we just reverse the order of layers: $(0, \dots, \nu) \mapsto (\nu, \dots, 0)$.

Equation (2.45) is a *split boundary problem* because the given amplitudes $t_0 = 1$, $r_\nu = 0$ appear on different sides of the equation. It can be reorganized as

$$\begin{pmatrix} t_\nu \\ r_0 \end{pmatrix} = W \begin{pmatrix} 1 \\ 0 \end{pmatrix} \quad (2.47) \quad \{\{EW1f\}\}$$

with

$$W = \mathcal{W}(M) := \begin{pmatrix} M_{tt}^{-1} & M_{tt}^{-1}M_{tr} \\ M_{rt}M_{tt}^{-1} & (M_{rr} - M_{rt}M_{tt}^{-1}M_{tr}) \end{pmatrix}. \quad (2.48) \quad \{\{EM2W\}\}$$

For later use, we note the inverse function

$$M = \mathcal{M}(W) = \begin{pmatrix} (W_{tt} - W_{tr}W_{rr}^{-1}W_{rt}) & W_{tr}W_{rr}^{-1} \\ W_{rr}^{-1}W_{rt} & W_{rr}^{-1} \end{pmatrix}. \quad (2.49) \quad \{\{EW2M\}\}$$

This formalism, originally developed for dynamic X-ray diffraction [15, 16], holds also if the matrix components are not commutative under multiplication. This will allow us later (for polarized neutrons, Chapter 4) to replace the scalar matrix components by 2×2 matrices.

From (2.47) and (2.48), we can read off

$$t_\nu = M_{tt}^{-1} \quad \text{and} \quad r_0 = M_{rt}M_{tt}^{-1}. \quad (2.50) \quad \{\{Etfri0J\}\}$$

With this, the split boundary problem is formally solved. However, the matrix product M (2.46) is numerically unstable [16, Sects. III, IV]. Therefore, the actual computation of r_0 and t_ν is done through a recursion (Sec. 2.2.2, TODO: polarized case).

If there is one single interface ($\nu = 1$), then $M = S_1$ yields the standard Fresnel results, namely the transmitted amplitude

$$t_1 = \frac{2\kappa_0}{\kappa_0 + \kappa_1} \quad (2.51) \quad \{\{\text{EtFresnel}\}\}$$

and the reflected amplitude

$$r_0 = \frac{\kappa_0 - \kappa_1}{\kappa_0 + \kappa_1}. \quad (2.52) \quad \{\{\text{ErFresnel}\}\}$$

2.2.2 Recursive solution

{Srt1}

As mentioned under (2.50), the matrix product M (2.46) is numerically unstable [16, Sects. III, IV]. It is therefore preferable to solve the split boundary problem through a recursion.² Also, to compute scattering it is not sufficient to determine r_0 and t_ν ; the radiation amplitudes inside the inner layers are also needed. This is another good reason to use a recursive algorithm.

In the polarized case, we will use a recursion based on the matrix inversion (2.49) (TODO: confirm and insert link to section). In the scalar case, we use the much simpler recursion of Parratt [17]. It is based on the insight that one does not need to compute t_l and r_l separately, but only their ratio $x_l := r_l/t_l$. Spelling out (2.39) with $\delta := \delta_{l-1}$ and $s^\pm := s_l^\pm$, we obtain

$$x_{l-1} = \frac{\delta s^- + \delta s^+ x_l}{\delta^{-1} s^+ + \delta^{-1} s^- x_l} = \delta^2 \frac{R + x_l}{1 + R x_l}. \quad (2.53) \quad \{\{\text{EParratt}\}\}$$

The second expression involves the single-interface Fresnel reflection coefficient

$$R := \frac{s^-}{s^+} = \frac{\kappa_{l-1} - \kappa_l}{\kappa_{l-1} + \kappa_l}. \quad (2.54) \quad \{\{\text{EParratt}\}\}$$

The recursion starts at the bottom with $x_\nu = 0$.

²In early versions of BornAgain, we started from the bottom with $\tilde{t}_\nu = 1$, and normalized the final result by division through \tilde{t}_0 . For opaque samples, this algorithm fails because of arithmetic overflow. Through some versions of BornAgain, we used bisection to search for the bottom-most layer with finite transmitted intensity. Then we noted that the simple recursion can be rescued by renormalizing after each step. This turned out to be equivalent to the Parratt recursion [17].

2.3 Implementation

{SimplML}

Last updated to reflect the actual code in May 2023.

2.3.1 Call chain

All simulations are run through the virtual function `ISimulation::runComputation`.

For classes `ScatteringSimulation` and `OffspecSimulation`, most work is done in `Compute::scattered_and_reflected`,

for class `SpecularSimulation` in `Compute::reflectedIntensity`,

whereas class `DepthprobeSimulation` performs the computation directly in `runComputation`.

In function `Compute::scattered_and_reflected`,

incoming and outgoing fluxes are obtained from functions `ReSample::fluxesIn` and `fluxesOut`, and stored in instances of class `Fluxes`, which incarnates `OwningVector<IFlux>`.

Following that, scattering is computed by functions `Compute::dwbaContribution` and `Compute::roughMultiLayerContribution`.

Specular intensity is added to the appropriate detector pixel by function `Compute::gisasSpecularContribution`.

In `DepthprobeSimulation::runComputation`, incoming fluxes are obtained from function `ReSample::fluxesIn`.

In functions `ReSample::fluxesIn` and `fluxesOut` call either `Compute::SpecularScalar::fluxes` or `Compute::SpecularMagnetic::fluxes`.

For specular simulations, function `Compute::reflectedIntensity` calls either `Compute::SpecularScalar::topLayerR` or `Compute::SpecularMagnetic::topLayerR`. These functions only return amplitudes reflected from the top of the sample, whereas the `fluxes` functions called for scattering or depthprobe simulation compute up and down travelling amplitudes for each sample layer.

Functions `fluxes` and `topLayerR` are implemented in files [ComputeFluxScalar.cpp](#) and [ComputeFluxMagnetic.cpp](#), where they share some local functions.

2.3.2 Scalar fluxes

The core numeric algorithm for the scalar flux computation is implemented in [ComputeFluxScalar.cpp](#). Here the code is simplified by omitting roughness and transmission geometry. The code uses class `Spinor`, which has components `u` and `v`, here representing transmitted and reflected amplitude. Interfaces are numbered as in Fig. 2.2.

```

1  std::vector<Spinor>
2  computeTR(SliceStack& slices, std::vector<cmplx>& kz)
3  {
4      // Parratt algorithm, pass 1:
5      //   compute t/t factors and r/t ratios from bottom to top.
6      size_t N = slices.size();
7      std::vector<cmplx> tfactor(N-1); // transmission damping
8      std::vector<cmplx> ratio(N);    // Parratt's x=r/t
9      ratio[N-1] = 0;
10     for (size_t i = N-1; i > 0; i--) {
11         cmplx slp = 1 + kz[i]/kz[i-1];
12         cmplx slm = 1 - kz[i]/kz[i-1];
13         cmplx delta = exp_I(kz[i-1] * slices[i-1].thicknessOr0());
14         cmplx f = delta / (slp + slm * ratio[i]);
15         tfactor[i-1] = 2 * f;
16         ratio[i-1] = delta * (slm + slp * ratio[i]) * f;
17     }
18
19     // Parrat algorithm, pass 2:
20     //   compute r and t from top to bottom.
21     std::vector<Spinor> TR(N);
22     TR[0] = Spinor(1., ratio[0]);
23     for (size_t i = 1; i < N; ++i) {
24         TR[i].u = TR[i-1].u * tfactor[i-1]; // Spinor.u is t
25         TR[i].v = ratio[i] * TR[i].u;       // Spinor.v is r
26     }
27
28     return TR;
29 }

```

{Lti}

{Lri}

There are two code blocks, each with a loop over interfaces. The first loop runs from bottom $l = \nu$ to top $l = 1$. Variables `slp` and `slm` are the coefficients s_l^\pm of (2.43). Variable `delta` is δ_{l-1} as defined in (2.36). These are used for recursively computing transmission damping factors

$$F_{l-1} := \frac{2\delta_{l-1}}{s_l^+ + s_l^- x_l} \quad (2.55)$$

and Parratt ratios (2.53)

$$x_{l-1} = \delta_{l-1} \frac{s_l^- + s_l^+ x_l}{2} F_{l-1} = \delta_{l-1}^2 \frac{s_l^- + s_l^+ x_l}{s_l^+ + s_l^- x_l}, \quad (2.56)$$

starting from the bottom value $x_\nu = 0$. The second loop starts from the top where $t_0 = 1, r_0 = 0$. From (2.39),

$$t_{l-1} = \delta^{-1} \left(\frac{s^+}{2} t_l + \frac{s^-}{2} r_l \right) = \frac{s^+ + s^- x_l}{2\delta} t_l = F_{l-1}^{-1} t_l. \quad (2.57)$$

Bringing F_{l-1} to the other side, we obtain code line 24. By definition, $x_l = r_l/t_l$. Bringing t_l to the other side, we obtain code line 25.

2.4 Vanishing vertical wavenumber, evanescent case etc

The above algorithm fails if $\kappa_{l-1} \rightarrow 0$ because M_l becomes singular.

TODO: revise the outcommented text in this section

3 Scattering by rough interfaces

{SRough}

The SLD decomposition (2.1) leaves some freedom how to model interface roughness. In the standard approach, $\bar{v}(z)$ always represents the average SLD at given height z . Insofar, roughness has the same effect as an SLD gradient in a sample that is translationally invariant in the xy plane. The effect of graded SLD profiles upon reflection and transmission of a multilayer sample is discussed in Sec. 3.1.

Additionally, the horizontal inhomogeneity of a rough interface gives rise to diffuse scattering, discussed in Sec. 3.2.

By energy conservation, scattering reduces the reflected or/and transmitted intensity. How to account for these losses in the R/T computation is an open research question (TODO: link to section).

3.1 Propagation through graded interfaces

{Sgraded}

3.1.1 Interface with tanh profile

Graded interfaces have a smooth SLD profile, i.e. the function $\bar{v}(z)$ or $\kappa^2(z)$ evolves continuously from one bulk value to the other. Among the SLD profiles that can be solved analytically, the tanh (Fig. 3.1a) profile is particularly important. A good summary of the solution can be found in Ch. 2.5 of Lekner [18].¹ Whereas Lekner only considers the electromagnetic case with a profile $\epsilon(z)$, we summarize the theory in terms of $\kappa = \epsilon K^2 - k_{\parallel}^2$.

We posit a profile

$$\kappa^2(z) = \frac{\kappa_a^2 + \kappa_b^2}{2} + \frac{\kappa_b^2 - \kappa_a^2}{2} \tanh \frac{z}{2\tau}. \quad (3.1)$$

The parameter τ is related to the roughness length σ of the BornAgain API through

$$\pi\tau = \left(\frac{\pi}{2}\right)^{3/2} \sigma. \quad (3.2)$$

For reference, we note the derivative

$$\frac{d}{dz} \kappa^2(z) = \frac{\kappa_b^2 - \kappa_a^2}{4\tau} \cosh^{-2} \frac{z}{2\tau}. \quad (3.3)$$

¹He credits Eckart (1930) and Epstein (1930) for the solution. For a short summary, see also [19, § 25, exercise 3].

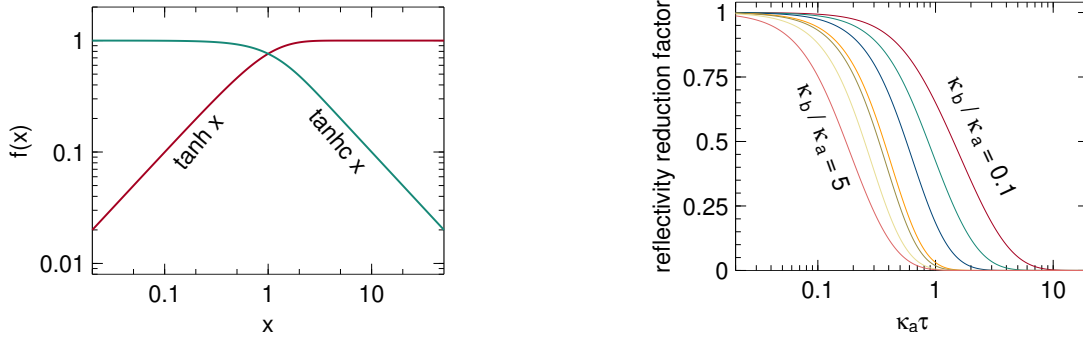


Figure 3.1: (a) Functions \tanh and \tanhc . (b) Reflectivity reduction factor, obtained by dividing (3.7) through the Fresnel reflectivity (2.51), as function of $\kappa_a \tau$ for ratios κ_b/κ_a of 0.1, 0.2, 0.4, 0.9, 1.1, 2, and 5.

{Ftanhc}

The solution $\Phi(z)$ involves a hypergeometric function. Here we only note the reflection coefficient [18, Eq. 2.88]

$$r_{ab} = e^{2i\varphi} \frac{\sinh \pi \tau (\kappa_a - \kappa_b)}{\sinh \pi \tau (\kappa_a + \kappa_b)}. \quad (3.4) \quad \{\text{ErTanh}\}$$

The phase φ is a real number as long as κ_a and κ_b are real. The transmission coefficient t_{ab} is communicated in [20]. Using various properties of the Gamma and sinh functions, one can verify flux conservation (2.44).

In the limit $\tau \rightarrow 0$, the phase factor φ in (3.4) goes to zero. For simplicity, we let $\varphi = 0$ throughout. This approximation is equivalent to an adjustment of the interface position z_{ab} by an amount that can be expected to be small compared to the interface thickness τ_{ab} .

To rewrite (3.4) in a form inspired by the Fresnel reflection coefficient (2.52), we use the identity

$$\frac{\sinh(x - y)}{\sinh(x + y)} = \frac{\sinh x \cosh y - \sinh y \cosh x}{\sinh x \cosh y + \sinh y \cosh x} = \frac{\tanh y - \tanh x}{\tanh y + \tanh x} \quad (3.5) \quad \{\text{ErTanh}\}$$

with $x := \pi \tau \kappa_a$ and $y := \pi \tau \kappa_b$. We write $\tanhc x := (\tanh x)/x$ (Fig. 3.1a) and define the roughness factor

$$\mathcal{R}_{ab} := \sqrt{\frac{\tanhc \pi \tau \kappa_b}{\tanhc \pi \tau \kappa_a}}. \quad (3.6) \quad \{\text{ERba}\}$$

With all this, (3.4) can be cast as

$$r_{ab} = \frac{\mathcal{R}_{ab}^{-1} \kappa_a - \mathcal{R}_{ab} \kappa_b}{\mathcal{R}_{ab}^{-1} \kappa_a + \mathcal{R}_{ab} \kappa_b}, \quad (3.7) \quad \{\text{ErTanh2}\}$$

which has the form of the Fresnel reflection coefficient (2.52), except for the factors \mathcal{R}_{ab}^{-1} and \mathcal{R}_{ab} . For $\tau \rightarrow 0$, these factors go to 1 so that (2.52) is fully recovered (Fig. 3.1b).

The reduced r_{ab} of (3.7) can be obtained from the basic transfer matrix equation (2.39) if the coefficients s^\pm of (2.43) are replaced by²

$$s_a^\pm = \mathcal{R}_{ab}^{-1} \pm \mathcal{R}_{ab} \kappa_b / \kappa_a. \quad (3.8) \quad \{\{\text{Es1pmTanh}\}\}$$

It is easily verified that the energy conservation (2.44) still holds.

3.1.2 Névot-Croce factor

The Névot-Croce factor is an exponential attenuation factor for the reflection coefficient:

$$\tilde{r}_{ab} = r_{ab} e^{-2k_a k_b \sigma_{ab}^2}, \quad (3.9) \quad \{\{\text{ErNC}\}\}$$

where r_{ab} is the Fresnel reflectivity (2.52) of a sharp interface. This form can be obtained in various ways, with more or less hand-wavy arguments or approximations. As e.g. used by Tolan it can be obtained by averaging the Parrat recursion equations over a Gaussian material profile [21], equation 2.34. The same result can also be obtained from formal perturbation theory, see e.g. [22] and references therein.

If the transmission coefficients are left unaltered, the resulting reduction in reflectivity can be interpreted as a loss into diffuse scattering channels. This interpretation is mentioned by Névot et al. [23].

More questionable is the simultaneous modification of the transmission coefficient. Currently BornAgain uses

$$\tilde{t}_{ab} = t_{ab} e^{+(k_a - k_b)^2 \sigma^2 / 2}, \quad (3.10) \quad \{\{\text{EtNC}\}\}$$

where t_{ab} is the Fresnel coefficient (2.51). This is the result obtained by Tolan [21, Eq. 2.35], and is also given by de Boer [22] as a result from formal perturbation theory in the limit of very small lateral correlation length. To obtain \tilde{r}_{ab} and \tilde{t}_{ab} from the basic transfer matrix equation (2.39), we need to replace the coefficients s^\pm of (2.43) by

$$s_l^\pm = (1 \pm \kappa_{l-1} / \kappa_l) \exp(-(\kappa_{l-1} \mp \kappa_l)^2 \sigma^2 / 2), \quad (3.11) \quad \{\{\text{Es1pmNC}\}\}$$

which is consistent with [24, Eq. 3.114].

However, the total reflected and transmitted flux $\kappa_a |\tilde{r}_{ab}|^2 + \kappa_b |\tilde{t}_{ab}|^2$, computed as in (2.44), is *greater* than the incoming flux κ_a . This takes all credibility from (3.10) and (3.11).

²Implemented in file [ComputeFluxScalar.cpp](#), function `transition` [30may23].

3.2 Scattering by a rough interface

{Sroughscatter}

Fragmentary. With contributions by Randolf Beerwerth and Walter Van Herck.³

3.2.1 Scattering in DWBA

{SroughDWBA}

In first-order distorted-wave Born approximation (DWBA), the scattering cross section is given by

$$\frac{d\sigma}{d\Omega} = \left| \int d^3r \Psi_i^*(\mathbf{r}) V(\mathbf{r}) \Psi_f(\mathbf{r}) \right|^2 =: |\langle \Psi_i | V | \Psi_f \rangle_{\mathbf{r}}|^2, \quad (3.12) \quad \{\text{Ecross1}\}$$

where $V(\mathbf{r})$ is the deviation from a reference potential $V^0(z)$ that is used to compute the distorted wave function Ψ for given incident and final far-field wave vectors $\mathbf{k}_i, \mathbf{k}_f$. Since the distorted waves are governed by a mean potential that only depends on z , they have the form

$$\Psi(\mathbf{r}) = e^{i\mathbf{k}_{\parallel} \mathbf{r}_{\parallel}} \Phi(z). \quad (3.13) \quad \{\text{Ecross1}\}$$

We introduce the scattering vector

$$\mathbf{q} := \mathbf{k}_f - \mathbf{k}_i \quad (3.14)$$

and the vertically integrated form factor

$$F(\mathbf{r}_{\parallel}) := \int dz \Phi_i^*(z) V(\mathbf{r}) \Phi_f(z) =: \langle \Phi_i | V | \Phi_f \rangle_z \quad (3.15) \quad \{\text{DFpa}\}$$

so that we can write (3.12) as

$$\frac{d\sigma}{d\Omega} = \int d^2r'_{\parallel} \int d^2r_{\parallel} e^{i\mathbf{q}_{\parallel}(-\mathbf{r}'_{\parallel} + \mathbf{r}_{\parallel})} F^*(\mathbf{r}'_{\parallel}) F(\mathbf{r}_{\parallel}). \quad (3.16) \quad \{\text{Ecross11}\}$$

We recast (3.16) as a Fourier transform

$$\frac{d\sigma}{d\Omega} = A \int d^2r_{\parallel} e^{i\mathbf{q}_{\parallel} \mathbf{r}_{\parallel}} G(\mathbf{r}_{\parallel}) \quad (3.17) \quad \{\text{Ecross12}\}$$

with the illuminated area A and the spatial correlation function

$$G(\mathbf{r}_{\parallel}) := A^{-1} \int d^2r'_{\parallel} F^*(\mathbf{r}'_{\parallel}) F(\mathbf{r}'_{\parallel} + \mathbf{r}_{\parallel}). \quad (3.18) \quad \{\text{DGpa}\}$$

³Ingested from ba-intern/theory on 29may23. Material was originally Roughness.tex, then ch. 4 in Stratified.tex, then again in a separate document RoughScatter.tex.

3.2.2 Random potential

{Srandvar}

To describe disordered interfaces, we assume that the potential depends on a random variable $u(\mathbf{r}_{\parallel})$:

$$V(\mathbf{r}) = V(z; u(\mathbf{r}_{\parallel})). \quad (3.19) \quad \{\text{DGrpa}\}$$

The scattering cross section (3.12) must be replaced by an average over the function $u(\mathbf{r}_{\parallel})$,

$$\frac{d\sigma}{d\Omega} = \left\langle |\langle \Psi_i | V | \Psi_f \rangle_{\mathbf{r}}|^2 \right\rangle_{\{u\}}. \quad (3.20) \quad \{\{\text{Ecross2}\}\}$$

The subscripts \mathbf{r} and $\{u\}$ could help to distinguish the quantum-mechanical and the statistical average. However, to avoid overloaded notation, we will omit them in the following. Rather, we will always use big angular brackets to mark the statistical average.

The Fourier transformed cross section can be maintained as in (3.17) provided the spatial correlation function (3.18) is redefined as

$$G(\mathbf{r}_{\parallel}) := A^{-1} \int d^2 r'_{\parallel} \left\langle F^*(u(\mathbf{r}'_{\parallel})) F(u(\mathbf{r}'_{\parallel} + \mathbf{r}_{\parallel})) \right\rangle. \quad (3.21) \quad \{\{\text{D2Grpa}\}\}$$

We now assume that the distribution of the $u(\mathbf{r}'_{\parallel})$ and $u(\mathbf{r}'_{\parallel} + \mathbf{r}_{\parallel})$ depends only on the distance \mathbf{r}_{\parallel} , not on the absolute location \mathbf{r}'_{\parallel} . Thereby, Equation (3.21) can be simplified as

$$G(\mathbf{r}_{\parallel}) = \left\langle F^*(u(0)) F(u(\mathbf{r}_{\parallel})) \right\rangle. \quad (3.22) \quad \{\{\text{D2Grpa2}\}\}$$

The average involves a two-point correlation function $P_2(u, v; \mathbf{r}_{\parallel})$:

$$G(\mathbf{r}_{\parallel}) = \int du \int dv P_2(u, v; \mathbf{r}_{\parallel}) F^*(u) F(v). \quad (3.23) \quad \{\text{D2Grpa2}\}$$

We anticipate that the limiting behavior of P_2 is governed by the one-point distribution function P_1 ,

$$P_2(u, v; \mathbf{r}_{\parallel}) \rightarrow \begin{cases} P_1(u) \delta(u - v) & \text{for } \mathbf{r}_{\parallel} \rightarrow 0, \\ P_1(u) P_1(v) & \text{for } \mathbf{r}_{\parallel} \rightarrow \infty. \end{cases} \quad (3.24)$$

3.2.3 Covariance ex machina

{Scov}

In the pioneering paper by Sinha et al. [25] and in much of the subsequent literature [26], the scattering cross section is defined differently from Equation (3.20), namely as the covariance

$$\left. \frac{d\sigma}{d\Omega} \right|_{\text{cov}} := \text{Cov}_{\{u\}} \left(\langle \Psi_i | V | \Psi_f \rangle^*, \langle \Psi_i | V | \Psi_f \rangle \right) \equiv \left\langle |\langle \Psi_i | V | \Psi_f \rangle|^2 \right\rangle - \left| \left\langle \langle \Psi_i | V | \Psi_f \rangle \right\rangle \right|^2. \quad (3.25) \quad \{\{\text{DcrossCov}\}\}$$

To compensate for the negative extra term, there must be another cross section

$$\left. \frac{d\sigma}{d\Omega} \right|_{\text{T/R}} := \left| \left\langle \langle \Psi_i | V | \Psi_f \rangle \right\rangle \right|^2 \quad (3.26) \quad \{\{\text{DcrossRT}\}\}$$

$$= A \int d^2 r_{\parallel} e^{i\mathbf{q}_{\parallel} \mathbf{r}_{\parallel}} \left\langle F(0) \right\rangle^* \left\langle F(\mathbf{r}_{\parallel}) \right\rangle. \quad (3.27) \quad \{\text{DcrossRT}\}$$

The one-point averages are governed by the distribution function $P_1(u)$ that does not depend on horizontal location. Hence

$$\left. \frac{d\sigma}{d\Omega} \right|_{\text{T/R}} = A \int d^2 r_{\parallel} e^{i\mathbf{q}_{\parallel} \mathbf{r}_{\parallel}} \left| \left\langle F \right\rangle \right|^2 \quad (3.28) \quad \{\{\text{EcrossRT2}\}\}$$

$$= A(2\pi)^2 \delta(\mathbf{q}_{\parallel}) \left| \left\langle F \right\rangle \right|^2. \quad (3.29) \quad \{\text{EcrossRT2}\}$$

This cross section is only nonzero if $\mathbf{q}_{\parallel} = 0$. Elastic scattering must fulfill $k_f = k_i$. Together, these conditions imply $k_{iz} = \pm k_{fz}$, which is only satisfied by the direct (transmitted) and by the specular (reflected) beam. For this reason, the cross section (3.26) has been labelled “R/T”.

In the present context, we are only interested in scattering out of the transmitted or reflected beam. Therefore we can ignore the R/T cross section (3.26), and substitute the covariance (3.25) for the original cross section (3.12). We will see that this simplifies computations. So we replace (3.17) by

$$\left. \frac{d\sigma}{d\Omega} \right|_{\text{T/R}} = A \int d^2 r_{\parallel} e^{i\mathbf{q}_{\parallel} \mathbf{r}_{\parallel}} \Delta G(\mathbf{r}_{\parallel}) \quad (3.30) \quad \{\{\text{EcrossDG}\}\}$$

with the modified correlation function (3.22)

$$\Delta G(\mathbf{r}_{\parallel}) := \text{Cov}\left(F^*(u(0)), F(u(\mathbf{r}_{\parallel}))\right) \quad (3.31) \quad \{\{\text{DDGrpa}\}\}$$

$$= \int du \int dv \Delta P_2(u, v; \mathbf{r}_{\parallel}) F^*(u) F(v). \quad (3.32) \quad \{\text{DDGrpa}\}$$

The integral involves the distribution function

$$\Delta P_2(u, v) := P_2(u, v) - P_1(u)P_1(v). \quad (3.33) \quad \{\{\text{DDP2}\}\}$$

3.2.4 Sharp, rough interface

\{\{\text{Sinterface}\}\}

We consider a sharp transition between two different materials that takes place at a rough interface located at height $z = u(\mathbf{r}_{\parallel})$. The scattering potential is the difference

$$V(\mathbf{r}) = V_u(z; u(\mathbf{r}_{\parallel})) - V^0(z) \quad (3.34) \quad \{\{\text{EVasdiff}\}\}$$

between the actual potential for a given interface profile u

$$V_u(z; u) := \frac{V_a + V_b}{2} + \frac{V_a - V_b}{2} \text{sgn}(z - u) \quad (3.35) \quad \{\text{EVasdiff}\}$$

and the reference potential

$$V^0(z) := \frac{V_a + V_b}{2} + \frac{V_a - V_b}{2} s_0(z) \quad (3.36)$$

that has been used to compute the vertical wave functions Φ_i, Φ_f , and therefore does not contribute to scattering. The constants V_a, V_b are the values of V^0 in the bulk *above* and *below* the interface, denoted by layer indices a and b. The profile function $s_0(z)$ has the limits $s_0(\pm\infty) = \pm 1$. We rewrite (3.34) as

$$V(\mathbf{r}) = (V_b - V_a) \mathcal{V}(z; u(\mathbf{r}_{\parallel})) \quad (3.37)$$

with the dimensionless difference potential

$$\mathcal{V}(z, u) := \frac{1}{2} [\text{sgn}(z - u) - s_0(z)]. \quad (3.38) \quad \{\text{DVddp}\}$$

To get rid of a constant prefactor, we rewrite the correlation function (3.31) as

$$\Delta G(\mathbf{r}_{\parallel}) = |V_b - V_a|^2 \Delta g(\mathbf{r}_{\parallel}) \quad (3.39) \quad \{\text{E31Grpa}\}$$

with the reduced correlation function

$$\Delta g(\mathbf{r}_{\parallel}) := \text{Cov}\left(f^*(u(0)), f(u(\mathbf{r}_{\parallel}))\right) = \int du \int dv \Delta P_2(u, v; \mathbf{r}_{\parallel}) f^*(u) f(v) \quad (3.40) \quad \{\text{DDgrpa}\}$$

and the reduced vertical form factor

$$f(u) := \int dz \Phi_i^*(z) \mathcal{V}(z; u) \Phi_f(z). \quad (3.41) \quad \{\text{Dfpa}\}$$

3.2.5 Stepwise reference potential

To facilitate computations, we approximate the smooth function $s_0(z)$ by a step function that takes J different values s_j , with layer index j running from $b = 1$ to $a = J$. We decompose the vertical wave function Φ_d (with $d = i, f$) as

$\{\text{Sstepwise}\}$

$$\Phi_d(z) = \sum_{j=1}^J [z \in \mathcal{L}_j] \Phi_{dj}(z), \quad (3.42) \quad \{\text{Dfpa}\}$$

where \mathcal{L}_j denotes the z interval occupied by layer j . Within one layer, the vertical wave function consists of two exponentials with constant coefficients,

$$\Phi_{dj}(z) = t_{dj} e^{-i\kappa_{dj} z} + r_{dj} e^{i\kappa_{dj} z}. \quad (3.43) \quad \{\text{2EPhijz}\}$$

To prepare for summation over downward and upward travelling waves, we rewrite (3.43) as

$$\Phi_{dj}(z) = \sum_{\alpha=-1, +1} c_{dj\alpha} e^{i\kappa_{dj\alpha} z} \quad (3.44) \quad \{\text{EPhidj}\}$$

with $c_{dj-} := t_{dj}$, $c_{dj+} := r_{dj}$, and $\kappa_{j\pm} := \pm\kappa_j$. With the further definitions

$$q_{j\alpha\beta} := \kappa_{fj\alpha} - \kappa_{ij\beta}, \quad (3.45)$$

$$B_{j\alpha\beta} := c_{ij\alpha}^* c_{fj\beta}, \quad (3.46)$$

the wave function product in (3.41) becomes

$$\Phi_i^*(z)\Phi_f(z) = \sum_j [z \in \mathcal{L}_j] \sum_{\alpha}^{-,+} \sum_{\beta}^{-,+} B_{j\alpha\beta} e^{iq_{j\alpha\beta}z}. \quad (3.47)$$

Diffuse scattering is governed by the dimensionless difference potential (3.38), which can be written

$$\mathcal{V}(z, u) := \frac{1}{2} [\text{sgn}(z - u) - s_{j(z)}] \quad (3.48) \quad \{\text{EVddpstep}\}$$

with a function $j(z)$ that yields the layer index for a given vertical coordinate z .

3.2.6 One-step reference potential

\{\text{Sonestep}\}

We now choose a reference potential that has a single step at $z = 0$. In this case, the profile function is just $s_0(z) = \text{sgn}(z)$. The dimensionless difference potential (3.38) and (3.48) can be further simplified to take the form

$$\mathcal{V}(z; u) = [0 < z < u] - [u < z < 0], \quad (3.49) \quad \{\text{EVddpstep}\}$$

with the Iverson-Knuth indicator bracket defined by $[\text{false}] = 0$ and $[\text{true}] = 1$. After some rearrangement we find

$$f(u) = \sum_j^{\text{b,a}} [u \in \mathcal{L}_j] \sum_{\alpha}^{-,+} \sum_{\beta}^{-,+} B_{j\alpha\beta} \int_0^u dz e^{iq_{j\alpha\beta}z}. \quad (3.50) \quad \{\text{Efujab}\}$$

From here on, it is convenient to work with a bundled index $\mu \equiv (\alpha, \beta)$ that runs from 0 to 3 and stands for the four possible combinations of $\pm\pm$. With the further abbreviation

$$A_{j\mu} := B_{j\mu}/q_{j\mu}, \quad (3.51) \quad \{\text{DA}\}$$

the result of carrying out the integral in (3.50) can be written as

$$f(u) = \sum_j^{\text{b,a}} [u \in \mathcal{L}_j] \sum_{\mu}^{\pm\pm} \frac{A_{j\mu}}{i} (e^{iq_{j\mu}u} - 1). \quad (3.52) \quad \{\text{DA}\}$$

The reduced correlation function (3.40) is just the covariance of $f^*(u(0))$ and $f(u(\mathbf{r}_{\parallel}))$. Only terms that involve both $u(0)$ and $u(\mathbf{r}_{\parallel})$ contribute. This leaves us with

$$\Delta g(\mathbf{r}_{\parallel}) = \sum_j^{\text{b,a}} \sum_k^{\text{b,a}} \sum_{\mu}^{\pm\pm} \sum_{\nu}^{\pm\pm} A_{j\mu}^* A_{k\nu} D_{j\mu, k\nu}(\mathbf{r}_{\parallel}) \quad (3.53) \quad \{\text{EDgrpa1}\}$$

with

$$D_{j\mu,k\nu}(\mathbf{r}_{\parallel}) := \int_{\mathcal{L}_j} du \int_{\mathcal{L}_k} dv \Delta P_2(u, v; \mathbf{r}_{\parallel}) e^{-iq_{j\mu}u + iq_{k\nu}v}. \quad (3.54) \quad \{\text{DD4}\}$$

If the vertical scattering wavenumbers q are real, then $D_{j\mu,k\nu}^* = D_{k\nu,j\mu}$. This allow us to compute (3.53) as

$$\Delta g(\mathbf{r}_{\parallel}) = \sum_{j\mu} |A_{j\mu}|^2 D_{j\mu,j\mu}(\mathbf{r}_{\parallel}) + \sum_{j\mu < k\nu} 2\text{Re } A_{j\mu}^* A_{k\nu} D_{j\mu,k\nu}(\mathbf{r}_{\parallel}). \quad (3.55) \quad \{\text{EDgrpa1c}\}$$

The operator $<$ under the second sum refers to some lexical ordering of the indices that is used to preclude double counts.

3.2.7 Gaussian roughness

\{\text{SGauss}\}

From this point on, we assume a specific distribution function P_2 , namely a bivariate normal distribution [27]. For brevity, we shall use the standard normal distribution

$$N_1(X) := \frac{1}{\sqrt{2\pi}} \exp\left(-\frac{X^2}{2}\right), \quad (3.56) \quad \{\text{EDgrpa1c}\}$$

and the standard bivariate normal distribution [27]

$$N_2(X, Y; \rho) := \frac{1}{2\pi\sqrt{1-\rho^2}} \exp\left[-\frac{X^2 + Y^2 - 2\rho XY}{2(1-\rho^2)}\right] \quad (3.57) \quad \{\text{DN2}\}$$

$$= N_1\left(\frac{Y+X}{\sqrt{2(1+\rho)}}\right) N_1\left(\frac{Y-X}{\sqrt{2(1-\rho)}}\right) \quad (3.58) \quad \{\text{EN2fac}\}$$

with $\rho < 1$. For $\rho \rightarrow 1$, one can see from (3.58) that $N_2(X, Y)$ goes to $N_1(X)\delta(X-Y)$. We now choose

$$P_1(u) := N_1\left(\frac{u}{\sigma}\right) \quad (3.59) \quad \{\text{EN2fac}\}$$

and

$$P_2(u, v; \mathbf{r}_{\parallel}) := N_2\left(\frac{u}{\sigma}, \frac{v}{\sigma}; \rho(\mathbf{r}_{\parallel})\right). \quad (3.60)$$

The standard deviation σ characterizes the vertical extent of interface fluctuations. It is undifficult to verify that

$$\int dv P_2(u, v; \mathbf{r}_{\parallel}) = P_1(u) \quad (3.61)$$

for whatever $\rho(\mathbf{r}_{\parallel})$. Physics dictates that $0 \leq \rho(\mathbf{r}_{\parallel}) < 1$ for $\mathbf{r}_{\parallel} \neq 0$, and $\rho(0) = 1$. A specific horizontal correlation function $\rho(\mathbf{r}_{\parallel})$ will be chosen later.

The covariance distribution function (3.33) is given by

$$\Delta P_2(u, v; \mathbf{r}_{\parallel}) = \Delta N_2\left(\frac{u}{\sigma}, \frac{v}{\sigma}; \rho(\mathbf{r}_{\parallel})\right) \quad (3.62) \quad \{\text{EDP2}\}$$

with

$$\Delta N_2(X, Y; \rho) := N_2(X, Y; \rho) - N_1(X)N_1(Y) \quad (3.63)$$

$$\begin{aligned} &= N_1 \left(\frac{Y+X}{\sqrt{2(1+\rho)}} \right) N_1 \left(\frac{Y-X}{\sqrt{2(1-\rho)}} \right) \\ &\quad - N_1 \left(\frac{Y+X}{\sqrt{2}} \right) N_1 \left(\frac{Y-X}{\sqrt{2}} \right), \end{aligned} \quad (3.64) \quad \{\text{EDN2fac}\}$$

which has the small ρ expansion

$$\Delta N_2(X, Y; \rho) = N_1(X)N_1(Y) [\rho XY + \mathcal{O}(\rho^2)]. \quad (3.65) \quad \{\text{EDN2lin}\}$$

3.2.8 Analytic plane waves approximation

\{\text{SSinhaApprox}\}

The evaluation of the correlation function (3.53) can be simplified decisively if the wave functions Φ_d ($d = \text{i, f}$) in the vertical form factor (3.15) are approximated by two exponential functions with constant amplitudes. This amounts to omitting the j dependences in (3.44). In the literature, it is typically achieved by analytic continuation of the wavefunction of the upper layer, Φ_{da} , into the lower layer b, or vice versa. According to Pynn [28, p. 605], this approximation is implicit in the reflectivity theory of Névot and Croce [29]. Sinha et al. [25, following Eq. 4.37] introduced for the DWBA computation of diffuse scattering. Holý et al. [26] suggest to compute the scattering intensity twice, with Φ_{da} approximated by Φ_{db} , and vice versa. The approximation is valid if the two results agree within requested precision.

Under this assumption we can omit the layer index from B, q, A . The sums over j, k in (3.53) become trivial, the integrals over u, v are no longer restricted to layers, and the problem reduces to

$$\Delta g(\mathbf{r}_{\parallel}) = \sum_{\mu}^{\pm\pm} \sum_{\nu}^{\pm\pm} A_{\mu}^* A_{\nu} \int du \int dv \Delta P_2(u, v; \mathbf{r}_{\parallel}) e^{-iq_{\mu}u + iq_{\nu}v}. \quad (3.66) \quad \{\text{EDgrpaS1}\}$$

With (3.62) and (3.64), the solution is straightforward [25, Eq. 4.42]:

$$\Delta g(\mathbf{r}_{\parallel}) = \sum_{\mu}^{\pm\pm} \sum_{\nu}^{\pm\pm} A_{\mu}^* A_{\nu} \left[e^{\sigma^2 q_{\mu} q_{\nu} \rho(\mathbf{r}_{\parallel})} - 1 \right] e^{-\sigma^2 (q_{\mu}^2 + q_{\nu}^2)/2}. \quad (3.67) \quad \{\text{EDgrpaS2}\}$$

For small ρ , the difference in the bracket can be linearized in ρ . Recalling that $A = B/q$ (3.51), we obtain [25, Eq. 4.43]

$$\Delta g(\mathbf{r}_{\parallel}) \doteq \rho(\mathbf{r}_{\parallel}) \sigma^2 \sum_{\mu}^{\pm\pm} \sum_{\nu}^{\pm\pm} B_{\mu}^* B_{\nu} e^{-\sigma^2 (q_{\mu}^2 + q_{\nu}^2)/2}. \quad (3.68) \quad \{\text{EDgrpalin}\}$$

3.2.9 Refracted waves, linearized correlation

We now reconsider the problem of computing the correlation function (3.53) based on wave functions that account for refraction and reflection by the mean interface, and therefore are plane waves only within one layer. In other words, we proceed without Sinha's approximation of Section 3.2.8.

Instead, to make the problem computationally accessible, we use (3.65) to linearize in ρ from the onset. So approximate (3.54) as

$$D_{j\mu,k\nu}(\mathbf{r}_{\parallel}) \doteq \rho(\mathbf{r}_{\parallel}) \sigma^2 E_j^*(q_{j\mu}) E_k(q_{k\nu}) \quad (3.69) \quad \{\text{EDgrpa2}\}$$

with the shorthand

$$E_j(q) := \int_{\mathcal{L}_j} d\frac{u}{\sigma} N_1\left(\frac{u}{\sigma}\right) \frac{u}{\sigma} e^{iqu}. \quad (3.70) \quad \{\text{EDgrpa2}\}$$

Recall that j and k take the values b, a. The layers cover the semiinfinite intervals $\mathcal{L}_b = (-\infty, 0)$ and $\mathcal{L}_a = (0, \infty)$, hence

$$E_a(q) = \int_0^\infty dU N_1(U) U e^{iq\sigma U}, \quad E_b(q) = -E_a(-q). \quad (3.71)$$

Use partial integration to obtain

$$E_a(q) = \frac{1}{\sqrt{2\pi}} + \frac{iq\sigma}{2} \operatorname{erfcx}\left(\frac{-iq\sigma}{\sqrt{2}}\right), \quad (3.72)$$

$$E_b(q) = -\frac{1}{\sqrt{2\pi}} + \frac{iq\sigma}{2} \operatorname{erfcx}\left(\frac{iq\sigma}{\sqrt{2}}\right) \quad (3.73)$$

with the compensated complementary error function (function $w(iz)$ of Abramowitz and Stegun [30, 7.1.3])

$$\operatorname{erfcx}(z) := e^{z^2} \operatorname{erfc}(z). \quad (3.74)$$

If we make the additional assumption that B, q, A are layer independent, as in Sinha's plane-waves approximation, then it is straightforward to recover the linearized result (3.68) from the previous section.

3.2.10 Horizontal correlations

This is a verbatim copy of Sect. 5.6 from our reference paper [1], except for notes in boldface or italics.

The reduction of reflected and transmitted intensity is described by the Névot-Croce factor [29]. IsGISAXS supports this loss factor, but not the diffuse scattering.

In BornAgain, diffuse scattering and beam attenuation are computed consistently. **[Not yet! This needs urgently to be implemented.]** The roughness model is taken from Ref. [31]. The height h is assumed to be a Gaussian random variable. The correlation function at in-plane distance R is (I:21)

$$C(R) := \langle h(0)h(R) \rangle = \sigma^2 e^{-(R/\xi)^{2H}}. \quad (3.75)$$

This model has been introduced into the field of X-ray reflectivity by Sinha et al [25]. Compare their Eqns. 2.9 and 2.23.

The user needs to specify the amplitude σ , the correlation length ξ , and the Hurst parameter H . The latter is restricted to $0 < H \leq 1$. According to Ref. [31], it defines the fractal box dimension $D = 3 - H$ of the interface: The smaller H , the more jagged the interface (see Fig. I:7). *Again, the better reference is [25], and work cited therein.*

If there are two or more interfaces, then their height profiles may be correlated. Following again Ref. [31], this is specified through a vertical cross correlation length ξ_{\perp} that governs the correlations between two interfaces j and k , (I:22)

$$\langle h_j(0)h_k(R) \rangle = \frac{1}{2} \left[\frac{\sigma_k}{\sigma_j} C_j(R) + \frac{\sigma_j}{\sigma_k} C_k(R) \right] e^{-|z_j - z_k|/\xi_{\perp}}. \quad (3.76)$$

3.3 Literature review: reflectivity and scattering from rough surfaces

Scattering from a rough surface has been studied first at a macroscopic level, for sound and radar waves (see books in TUM OPAC; see references in [32]). For light scattering literature, see Refs. 1–26 in [33].

Steyerl 1972 [32]: First detailed discussion of neutron reflection from rough surfaces. Main application interest is total reflection in neutron guides. Unperturbed potential is step function. Wave equation in integral form; Green's functions, ascribed to saddle point method, appear in Eqns. 15,16 without derivation; explicit expressions for all four cases $z, z' \leq 0$ are given with some more computational details in [34, Eqn. 29]. Compact and credible expressions for upward and downward scattering in Eqns. 20,21. Result for reflected and transmitted intensity thoroughly analysed and criticised by Pynn [28]: neglect of phase factor makes approximation irrelevant for reflectometry.

Névot & Croce 1980 [29]: Experimental X-ray study. Highly cited. Attenuation of the reflected beam described by the *Névot-Croce factor* [Eqn. 3]. Theoretical section is hard to read; starts from previous results of Croce et al; claims to be self-consistent (auto-cohérente, p. 764). The key results of this work are rederived in much shorter, clearer, and more standard ways by Pynn [28] who also explicates which approximations were made.

Beckmann and Spizzichino 1987 [35]: Book about radar reflections; almost entirely concerned with wavelengths shorter than local radius of curvature, irrelevant for reflectometry [28].

Sinha et al 1988 [25]: Top-cited paper. Sects. II and III are in Born Approximation, with application e. g. to powders. Application to liquid interface. They consider only single interfaces. Grazing incidence and DWBA come in Sect. IV. For $q_z \geq q_c$, a small- q expansion reproduces the Névot-Croce factor. For $q_z < q_c$, on the other hand, $|R| < 1$ is not found: 1st-order DWBA violates the optical theorem; the 2nd order would be needed, but is not worked out. Pynn [28, Eqn. 10] criticizes the forward scattering term [25, Eqn. 4.12], which involves the wrong incoming eigenfunction (for the plane instead of the rough surface).

Pynn 1992 [28]: A critical review of previous work, especially Steyerl [32], Névot & Croce [29], and Sinha et al [25]. Névot & Croce got the reflectivity essentially right, except for reflection coefficients smaller than 10^{-5} [p. 605]. Also discusses correlated interfaces.

Holý & al 1993 [26]: Concerned with multilayer reflectivity and diffuse scattering. Very readable summary and extension of Sinha theory. They write the perturbation Hamiltonian of a multilayer system as a sum of single-layer contributions. This splits up into a sum of four terms, similar to the expression Walter uses. They have only four terms as they assume that the fields are identical directly below and above the interface. Walter drops this condition and hence gets twice the terms with different averaging below and above the interface. As a consequence of writing the Hamiltonian as a sum of single interface contributions, diffuse scattering leads to a double sum with the covariances appearing. Here correlation models come in. They

introduce two of them: one without and the second with vertical correlation.

Summarized and extended to periodic multilayers by Holý & Baumbach [36]. Holý & al also contributed to the book [37]; in particular, chapter 11 could be interesting.

de Boer 1994 [38]: Purely theoretical description of specular reflectivity on single rough interfaces. Second order DWBA calculations of the reflection and transmission coefficients in the T -matrix formalism. The resulting expressions include the lateral correlation and are shown to have the Névot-Croce factor as a limiting value for small correlation length (i.e. negligible diffuse scattering). For large correlation length, the Debye-Waller like factor is recovered, while for intermediate correlation length an interpolation factor needs to be evaluated. This factor includes a two-dimensional surface integral. For a suitably chosen correlation function, it can be reduced to a one-dimensional integral which facilitates numeric evaluation.

de Boer & Leenaers 1996 [22]: Survey article that briefly summarizes results from several other articles. Explains under which limiting conditions results are applicable. Gives formulae of the Fresnel coefficients for both reflection and transmission on a single interface. Névot-Croce recovered as limit of small correlation lengths, can also serve for multilayer calculations. This limit corresponds to weak scattering and can be compared to graded interfaces, i.e. the numerical approximation via Slicing that completely neglects diffuse scattering. Mentions DWBA leading to intensities greater than unity below the critical angle, introduce Rayleigh method to circumvent this. This leads to another expression for the Fresnel coefficients for large correlation lengths, that can also be applied to multilayers.

Introduce an expression for the Fresnel coefficients for intermediate correlation lengths, that relates to the lateral correlation function. Only approximately applicable to multilayers, give reference to other 1996 paper [39].

Suggest interpolation approach to treat the fields in the vicinity of an interface.

Suggest also other starting points for the perturbative approach, namely to use already corrected Fresnel coefficients or graded interfaces. Here, they specifically mention the tanh profile as implemented in BornAgain.

Other potentially interesting papers from the same author: [40] [38]

The lateral correlation function implemented in BornAgain is taken from the paper [41].

de Boer 1996 [39]: Deals with multilayers and considers the effects of roughness in both specular reflectivity and diffuse scattering. Employs the T -matrix formalism to compute corrections in the DWBA up to second order, rather hard to understand and result not easily usable (for me, rb). Uses flat interfaces as the starting point for perturbation theory in Section II and graded interfaces in Section III. The latter is rather vague and hard to grasp. Results are presented, dominantly for x-ray fluorescence.

Concludes that as a starting point for the DWBA graded interfaces should be used, if both the reflectivity as well as the roughness are reasonably large. Suggests an interpolation method for the fields as a starting point for the DWBA, as the field obtained from Névot-Croce factors are wrong in the vicinity of interfaces.

Claims that the second-order term for diffuse scattering is generally negligible, except when the reflectivity is large as well as for large lateral correlation length and roughness. For specular reflection, mentions the first and second order contribution to

be of the same order in the roughness and is hence only negligible for small roughnesses. However, stresses that the DWBA is only valid for small roughness values or far above the critical wave vector. Their way of extrapolating [38] the results is only valid for single interfaces or very large perpendicular correlation.

Also mentions that he is not aware of any samples, where the second order contribution has to be considered and that the theory is completely untested.

Caticha 1995 [42]: Studies graded interface with roughness.

Rauscher et al 1995 [43]: Combine the roughness theory of Sinha et al [25] with bulk density fluctuations for different geometries, thereby specializing the generic formalism of Dietrich and Haase [44].

Ogura & Takahashi 1996 [45]: Scattering and reflection from a random surface in the language of mathematical physics, using Itô stochastic functionals. The surface has 100% reflectance (Eqns. 3.9–10), so they miss the most difficult aspects of the problem. Possibly a starting base for collaboration with mathematical physicists; otherwise without practical value for us.

Toperverg et al 2000 [46]: A short note on the *optical theorem* that ensures energy conservation under reflection, transmission and scattering. The only cited literature is Sinha et al 1988 [25] and de Boer 1994–96 [38, 41, 39]. For second-order DWBA they refer to a preprint by Toperverg et al 1997 (request pending). This paper drew our attention to the optical theorem, but is most probably made obsolete by other publications that work out more details.

Fuji 2010: [47]: Seems to be the initial claim, that the Parrat formalism as it is currently used with roughness included in the Fresnel coefficients assumes flux conservation and hence cannot account for losses due to roughness. Detailed derivation of a modified Parrat formula that contains both Fresnel r and t coefficients. Gives examples where unphysically deep fringes are removed by their new formula. The same example does indeed seem to show weird behavior that depending on the amount of roughness deep minima change their position.

Fuji 2013: [48]: They derive (short) a different version of the the Parrat recursion which does not imply conservation of flux. The claim is that this reduces deep unphysical minima in Kissieg fringes when roughness is added.

Fujii 2014: [49]: Presents a modified version of the Parrat formula, that explicitly depends on the Fresnel *transmission* coefficients. If conservation of the flux is imposed, his formula reduces to the well-known Parrat formula, where only the Fresnel *reflection* coefficient is present. More mathematical derivation of the approach is presented in [48]. Numerical results are presented for an example, where the author shows that the usual formula yields very good results for roughness parameters that do not agree with independent experimental results (TEM). His modified formula yields good agreement with the independently verified roughness parameters. The applied transmission coefficients are given without much explanation, but the given expression kind of resembles the expressions given by Tolan [21] for the large correlation length limit.

Fujii 2015: [50]: Computes effective roughness factors, where the lateral correlation is considered. Obtains an expression that again resembles equations (2.40) and (2.41) in the book by Tolan[21], however, with an effective roughness. Claims good

agreement with AFM measurements.

Chukhovskii 2011 & 2012 [51, 52]: Claims that DWBA is inapplicable for large roughness rms σ . As an alternative, develops *self-consistent wave approximation* (SCWA). Starting from a Green function [51, Eqn. 4], the derivation of the scattering cross section [51, Eqn. 20] and of the reflected intensity [51, Eqn. 19] looks relatively straightforward. Subsequent averages of random functions for the standard Gaussian surface model, however, lead to very long expressions [51, Eqns. 22,23]. The optical theorem is only satisfied in the limit of large surface correlation lengths ($k\xi\vartheta^2 \gg 1$) [52].

TODO <https://doi.org/10.1107/S2053273315016666> (2015)

TODO <https://www.nature.com/articles/s41598-020-68326-2> (2020)

Chukhovskii & Roshchin 2015 [53]: Yet another alternative to DWBA: expansion in q-eigenfunctions of the plane-surface problem.

Maruyama, Yamazaki & Soyama 2018 [54]: Conference proceeding, where the authors present actual computational results applying the theory from de Boer [38, 39], i.e. DWBA in second order to the specular reflectivity of multilayers. Comparison to the Névot-Croce factor, as well as contributions of the first and second order perturbation contribution. Their chosen example is very close to the Ti-Ni multilayer sample that was often considered by BA team members so far and could serve as an interesting test case for testing and comparing numerical results.

Hafner 2019 [55]: Contains simulations and experimental data of off-specular simulations where the contributions from specular reflection and scattering are put on a common scale. Cross sections are incoherently added, with geometric corrections arising from detector resolution and spread in angles/wavelengths. Mentions approximation valid for small scattered intensities. Summarizes statistical treatment of rough interfaces, similar correlation approach as in BornAgain.

4 Polarized wave propagation and scattering

{SPol}

In this chapter, we generalize our treatment of wave propagation and grazing-incidence small-angle scattering to polarized neutrons. We therefore need to study spinor wave equations, in contrast to the scalar theory of the previous chapter.

4.1 Polarized neutrons

{Snpol}

This section was outcommented in the “Physics Manual”. Restored 29may23.

4.1.1 Wave equation and propagation within one layer

To allow for polarization-dependent interactions, we replace the squared index of refraction n^2 by $1 + \underline{\underline{\chi}}$, where $\underline{\underline{\chi}}$ is a 2×2 susceptibility matrix. The wave equation ?? for layer l becomes

$$(\Delta + K^2 + K^2 \underline{\underline{\chi}}_l) \underline{\psi}(\mathbf{r}) = 0, \quad (4.1) \quad \{\text{Ewaveqp}\}$$

where $\underline{\psi}(\mathbf{r})$ is a two-component spinor wavefunction, with components $\psi_\uparrow(\mathbf{r})$ and $\psi_\downarrow(\mathbf{r})$. At interfaces between layers, both spinor components of $\underline{\psi}(\mathbf{r})$ and $\nabla \underline{\psi}(\mathbf{r})$ must evolve continuously.

The reasons for the factorization (2.9) still apply, and so we can write

$$\underline{\psi}(\mathbf{r}) = \underline{\psi}(z) e^{i\mathbf{k}_\parallel \mathbf{r}_\parallel}. \quad (4.2) \quad \{\text{Ewave3p}\}$$

As before, \mathbf{k}_\parallel is constant across layers. The wave equation (4.1) reduces to

$$\left(\partial_z^2 + K^2 + K^2 \underline{\underline{\chi}}_l - k_\parallel^2 \right) \underline{\psi}(z) = 0. \quad (4.3) \quad \{\text{Ewavezp}\}$$

We abbreviate

$$\underline{\underline{H}}_l := K^2(1 + \underline{\underline{\chi}}_l) - k_\parallel^2 \quad (4.4) \quad \{\text{Ewavezp}\}$$

so that the wave equation becomes simply

$$\left(\partial_z^2 + \underline{\underline{H}}_l \right) \underline{\psi}(z) = 0. \quad (4.5) \quad \{\text{Ewaveqp2}\}$$

The solution is

$$\underline{\psi}(z) = \sum_{k=1}^2 \underline{x}_{lk} \left(\alpha_{lk} e^{ip_{lk}(z-z_k)} + \beta_{lk} e^{-ip_{lk}(z-z_k)} \right), \quad (4.6) \quad \{\text{Epsizp}\}$$

where the \underline{x}_{lk} are eigenvectors of $\underline{\underline{H}}_l$ with eigenvalues p_{lk}^2 :

$$\left(-p_{lk}^2 + \underline{\underline{H}}_l\right) \underline{x}_{lk} = 0 \quad \text{for } l = 1, 2. \quad (4.7) \quad \{\text{Epsizp}\}$$

In a reproducible algorithm, the eigenvectors \underline{x}_{lk} must be chosen according to some arbitrary normalization rule, for instance

$$|\underline{x}_{lk}| = 1, \quad x_{il\uparrow} \text{ real and nonnegative.} \quad (4.8)$$

Similarly, a rule is needed how to handle the case of one degenerate eigenvalue, which includes in particular the case of scalar interactions.

4.1.2 Wave propagation across layers

Generalizing Section 2.1.5, we introduce the coefficient vector

$$c_l := (\alpha_{l1}, \alpha_{l2}, \beta_{l1}, \beta_{l2})^T. \quad (4.9)$$

To match solutions for neighboring layers, continuity is requested for both spinorial components of $\underline{\psi}$ and $\nabla \underline{\psi}$. We have at the bottom of layer l

$$F_l c_l = F_{l+1} D_{l+1} c_{l+1}, \quad (4.10) \quad \{\text{EFcFDcp}\}$$

where the matrices are

$$F_l := \begin{pmatrix} x_{i1\uparrow} & x_{i2\uparrow} & x_{i1\uparrow} & x_{i2\uparrow} \\ x_{i1\downarrow} & x_{i2\downarrow} & x_{i1\downarrow} & x_{i2\downarrow} \\ x_{i1\uparrow} p_{l1} & x_{i2\uparrow} p_{l2} & -x_{i1\uparrow} p_{l1} & -x_{i2\uparrow} p_{l2} \\ x_{i1\downarrow} p_{l1} & x_{i2\downarrow} p_{l2} & -x_{i1\downarrow} p_{l1} & -x_{i2\downarrow} p_{l2} \end{pmatrix} \quad (4.11) \quad \{\text{EFcFDcp}\}$$

and

$$D_l := \text{diag}(\delta_{l1}, \delta_{l2}, \delta_{l1}^*, \delta_{l2}^*) \quad (4.12)$$

with the phase factor

$$\delta_{lk} := e^{ip_{lk} d_k}. \quad (4.13)$$

Note that matrix F_l has the block form

$$F_l = \begin{pmatrix} \underline{\underline{x}}_l & \underline{\underline{x}}_l \\ \underline{\underline{x}}_l \underline{\underline{P}}_l & -\underline{\underline{x}}_l \underline{\underline{P}}_l \end{pmatrix} = \underline{\underline{x}}_l \cdot \begin{pmatrix} \underline{\underline{1}} & \underline{\underline{1}} \\ \underline{\underline{P}}_l & -\underline{\underline{P}}_l \end{pmatrix}, \quad (4.14)$$

with

$$\underline{\underline{x}}_l := (\underline{x}_{l1}, \underline{x}_{l2}), \quad \underline{\underline{P}}_l := \text{diag}(p_{l1}, p_{l2}). \quad (4.15)$$

This facilitates the computation of the inverse

$$F_l^{-1} = \frac{1}{2} \begin{pmatrix} \underline{\underline{1}} & \underline{\underline{P}}_l^{-1} \\ \underline{\underline{1}} & -\underline{\underline{P}}_l^{-1} \end{pmatrix} \cdot \underline{\underline{x}}_l^{-1}, \quad (4.16)$$

which is needed for the transfer matrix M_l , defined as in (2.40). With the new meaning of c_l and M_l , the recursion (2.39) and the explicit solution ?? hold as derived above. To resolve ?? for the reflected amplitudes α_{0l} as function of the incident amplitudes β_{0l} , we choose the notations

$$\underline{\alpha}_l := \begin{pmatrix} \alpha_{l1} \\ \alpha_{l2} \end{pmatrix}, \quad \underline{\beta}_l := \begin{pmatrix} \beta_{l1} \\ \beta_{l2} \end{pmatrix}, \quad M := M_1 \dots M_N =: \begin{pmatrix} \underline{\underline{m}}_{11} & \underline{\underline{m}}_{12} \\ \underline{\underline{m}}_{21} & \underline{\underline{m}}_{22} \end{pmatrix}, \quad (4.17)$$

where the $\underline{\underline{m}}_{lk}$ are 2×2 matrices. Eq. ?? then takes the form

$$\begin{pmatrix} \underline{\alpha}_0 \\ \underline{\beta}_0 \end{pmatrix} = \begin{pmatrix} \underline{\underline{m}}_{11} & \underline{\underline{m}}_{12} \\ \underline{\underline{m}}_{21} & \underline{\underline{m}}_{22} \end{pmatrix} \begin{pmatrix} \underline{0} \\ \underline{\beta}_N \end{pmatrix}, \quad (4.18)$$

which immediately yields

$$\underline{\alpha}_0 = \underline{\underline{m}}_{12} \underline{\underline{m}}_{22}^{-1} \underline{\beta}_0. \quad (4.19)$$

4.2 From old document “Reflectivity”

By choosing the convention that the plane of a multilayer lies within the x - y plane, and using the appropriate boundary conditions, the three-dimensional Helmholtz equation reduced to the usual one-dimensional Helmholtz equation $\hat{H}\Psi = 0$. Following [56] and [57], the Hamiltonian for a magnetized layer m in a sample is given by

$$\hat{H}_m = \frac{\partial^2}{\partial z^2} + k_0^2 - \frac{2\pi\hbar^2}{m_n} \left(b^N + b^M \vec{\sigma} \cdot \vec{b} \right) = \frac{\partial^2}{\partial z^2} + k_0^2 - 4\pi \underbrace{\left(\rho^N + \rho^M \vec{\sigma} \cdot \vec{b} \right)}_{\rho} = \frac{\partial^2}{\partial z^2} + p_m^2 \quad (4.20)$$

where \vec{b} is the unit vector of the magnetic field. Within this convention, the interaction is parametrized by the usual nuclear SLD ρ^N and the magnetic SLD ρ^M , which are both scalar quantities. For convenience, we then introduce the operator \hat{p}_m in layer m

$$\hat{p}_m := \frac{1}{2} \left((\lambda_+ + \lambda_-) + (\lambda_+ - \lambda_-) \vec{\sigma} \cdot \vec{b} \right), \quad (4.21)$$

with the eigenvalues given by

$$\lambda_{\pm} = \sqrt{k_0^2 - 4\pi (\rho^N \mp \rho^M)}. \quad (4.22)$$

The ansatz for the wave function is then

$$|\Psi_m(z)\rangle = \hat{S}_m(z) |\Psi_m(0)\rangle. \quad (4.23)$$

Here, the propagator \hat{S} is a 2×2 matrix given by the expression

$$\hat{S}(z) = \exp i\hat{p}_m(z - z_{m-1})\hat{t}_m + \exp -i\hat{p}_m(z - z_{m-1})\hat{r}_m, \quad (4.24)$$

and it propagates the wave function $|\Psi_m(0)\rangle$ at the bottom of layer m to position z . This notation is identical to the one introduced by [56] and [57] and \hat{t}_m and \hat{r}_m are operators that can be written as 2×2 matrices.

4.2.1 Transfer Matrix Method

For our purpose, it is instead more convenient to consider the two spinors $t_m = \hat{t}_m |\Psi_m(0)\rangle$ and $r_m = \hat{r}_m |\Psi_m(0)\rangle$. Analogously to the scalar case, these two spinors can be combined into a four-component vector $(t_m^T, r_m^T)^T$, so that the transition between interfaces m and $m+1$ can be described by the 4×4 transfer matrix

$$\begin{pmatrix} t_m \\ r_m \end{pmatrix} = \frac{1}{2} \begin{pmatrix} \delta^{-1} & 0 \\ 0 & \delta \end{pmatrix} \begin{pmatrix} 1 + p_m^{-1} p_{m+1} & 1 - p_m^{-1} p_{m+1} \\ 1 - p_m^{-1} p_{m+1} & 1 + p_m^{-1} p_{m+1} \end{pmatrix} \begin{pmatrix} t_{m+1} \\ r_{m+1} \end{pmatrix} \quad (4.25a)$$

$$= \frac{1}{2} \begin{pmatrix} \delta^{-1} & 0 \\ 0 & \delta \end{pmatrix} \begin{pmatrix} 1 + P & 1 - P \\ 1 - P & 1 + P \end{pmatrix} \begin{pmatrix} t_{m+1} \\ r_{m+1} \end{pmatrix}. \quad (4.25b)$$

{eq:interface_transfer_ma

Writing the reflectometry problem in this way for a multilayer that contains magnetic materials, allows to introduce structural roughness that is consistent with the scalar implementation in BornAgain. Due to the spinorial description of the amplitudes, the transfer matrix is now a 4×4 matrix. Analogously to the scalar case, we have defined the phase factor

$$\delta = \exp i p_m d_m, \quad (4.26) \quad \{\{\text{eq:polarized_transfer_m}\}\}$$

however, it is now a 2×2 matrix. In order to fully utilized the consistency with the scalar implementation we define that ratio $P = p_m^{-1} p_{m+1}$, which also turns into a 2 matrix.

4.2.1.1 Derivation

We consider a layer interface between layers $m + 1$ and m at position z_m . Therefore, we have $z_m - z_{m-1} = d_m$, the thickness of layer m .

We start from the ansatz for the wave functions in layers m and $m + 1$

$$\Psi_m(z) = \exp i \hat{p}_m (z - z_{m-1}) t_m + \exp -\hat{p}_m (z - z_{m-1}) r_m, \quad (4.27)$$

$$\Psi_{m+1}(z) = \exp i \hat{p}_{m+1} (z - z_m) t_{m+1} + \exp -i p_m (z - z_m) r_{m+1}. \quad (4.28)$$

Its derivatives are then given by

$$\frac{d\Psi_m}{dz} = i p_m \exp i p_m (z - z_{m-1}) t_m - i p_m \exp -i p_m (z - z_{m-1}) r_m \quad (4.29)$$

$$\frac{d\Psi_{m+1}}{dz} = i p_{m+1} \exp i p_{m+1} (z - z_m) t_{m+1} - i p_{m+1} \exp -i p_{m+1} (z - z_m) r_{m+1} \quad (4.30)$$

For convenience, we define $\varphi_m := p_m d_m$ and obtain from the boundary conditions $\Psi_m(z_m) = \Psi_{m+1}(z_m)$ and $d\Psi_m/dz(z_m) = d\Psi_{m+1}/dz(z_m)$

$$\exp i \varphi_m t_m + \exp -i \varphi_m r_m = t_{m+1} + r_{m+1} \quad (4.31) \quad \{\{\text{eq:boundary1}\}\}$$

$$p_m \exp i \varphi_m t_m - p_m \exp -i \varphi_m r_m = p_{m+1} t_{m+1} - p_{m+1} r_{m+1} \quad (4.32) \quad \{\{\text{eq:boundary2}\}\}$$

By multiplying (4.32) from the left with p_m^{-1} , we find

$$\exp i \varphi_m t_m - \exp -i \varphi_m r_m = p_m^{-1} p_{m+1} t_{m+1} - p_m^{-1} p_{m+1} r_{m+1}. \quad (4.33) \quad \{\{\text{eq:boundary2b}\}\}$$

Now from taking (4.31) + (4.33) and (4.31) - (4.33), we find

$$2 \exp i \varphi_m t_m = (1 + p_m^{-1} p_{m+1}) t_{m+1} + (1 - p_m^{-1} p_{m+1}) r_{m+1} \quad (4.34)$$

$$2 \exp -i \varphi_m r_m = (1 - p_m^{-1} p_{m+1}) t_{m+1} + (1 + p_m^{-1} p_{m+1}) r_{m+1} \quad (4.35)$$

Writing this as a single four-element vector yields

$$\begin{pmatrix} t_m \\ r_m \end{pmatrix} = \frac{1}{2} \begin{pmatrix} \exp -i \varphi_m & 0 \\ 0 & \exp i \varphi_m \end{pmatrix} \begin{pmatrix} (1 + p_m^{-1} p_{m+1}) t_{m+1} + (1 - p_m^{-1} p_{m+1}) r_{m+1} \\ (1 - p_m^{-1} p_{m+1}) t_{m+1} + (1 + p_m^{-1} p_{m+1}) r_{m+1} \end{pmatrix}. \quad (4.36) \quad \blacksquare$$

This is the desired representation of the transfer matrix given in equations (4.25).

4.2.2 Parratt Formalism

$$X_m = \hat{r}_m \hat{t}_m^{-1} \quad (4.37)$$

$$X_m = \exp ip_m d_m \tilde{X}_m \exp ip_m d_m \quad (4.38)$$

$$\tilde{X}_m = \frac{1 - p_m^{-1} p_{m+1} + (1 + p_m^{-1} p_{m+1}) X_{m+1}}{1 + p_m^{-1} p_{m+1} + (1 - p_m^{-1} p_{m+1}) X_{m+1}} \quad (4.39)$$

$$t_{m+1} = \frac{(1 + \tilde{X}_m) \exp ip_m d_m}{1 + X_{m+1}} t_m \quad (4.40)$$

- Kentzinger et al. introduce structural (nuclear) roughness into this formalism by adding Nevót-Croce factors to the operator $(1 - p_m^{-1} p_{m+1})$
- [57] mention the numerical stability of this algorithm due to the strictly positive imaginary parts in the phase factors
- Here X_m is a 2×2 operator

4.3 From old document “Stratified”

4.3.1 Wave equation and operator p

In the presence of magnetic interaction, the potential (1.28) has the z -dependent average

{Sopp}

$$\bar{v}(z) = \bar{v}_{\text{nucl}}(z) + \bar{v}_{\text{magn}}(z) \mathbf{e}_{\mathbf{B}} \underline{\underline{\sigma}}, \quad (4.41)$$

which involves the nuclear potential $v_{\text{nucl}}(\mathbf{r})$, the magnitude of the magnetic potential,

$$v_{\text{magn}}(\mathbf{r}) = \frac{m\mu}{2\pi\hbar^2} B(\mathbf{r}), \quad (4.42)$$

the neutron mass m , the neutron magnetic moment μ , the magnetic induction \mathbf{B} (with magnitude B and direction unit vector $\mathbf{e}_{\mathbf{B}}$), and the Pauli vector $\underline{\underline{\sigma}}$. Spinors, like the field $\underline{\Phi}(z)$, shall be underlined; 2×2 matrices that operate on spinors are underlined twice.

We redefine the vertical wave number κ , introduced in ??, to account only for the nuclear potential,

$$\kappa^2(z) := k_{\perp}^2(z) := K^2 - k_{\parallel}^2 - 4\pi\bar{v}_{\text{nucl}}(z), \quad (4.43) \quad \{\{\text{EkperpP}\}\}$$

whereas the wave equation ?? shall be replaced by

$$\left(\partial_z^2 + \underline{\underline{p}}^2(z) \right) \underline{\Phi}(z) = 0 \quad (4.44) \quad \{\{\text{EwzP}\}\}$$

with $\underline{\underline{p}}^2 := \kappa^2 - 4\pi\bar{v}_{\text{magn}}(z) \mathbf{e}_{\mathbf{B}} \underline{\underline{\sigma}}$. With [19, § 55, Exercice 1, p. 198], we find the operator¹

$$\underline{\underline{p}}(z) = \sqrt{\underline{\underline{p}}^2} = \frac{1}{2} [(\lambda_+ + \lambda_-) + (\lambda_+ - \lambda_-) \mathbf{e}_{\mathbf{B}} \underline{\underline{\sigma}}], \quad (4.45) \quad \{\{\text{EPauliRep}\}\}$$

expressed through its eigenvalues

$$\lambda_{\pm}(z) := \sqrt{\kappa^2(z) \mp 4\pi\bar{v}_{\text{magn}}(z)}. \quad (4.46) \quad \{\{\text{EPauliRep}\}\}$$

For future reference, we note the inverse operator²

$$\underline{\underline{p}}^{-1}(z) := \frac{1}{2\lambda_+\lambda_-} [(\lambda_+ + \lambda_-) - (\lambda_+ - \lambda_-) \mathbf{e}_{\mathbf{B}} \underline{\underline{\sigma}}]. \quad (4.47)$$

¹Implemented in `MatrixRTCoefficients::computeP()`.

²Implemented in `MatrixRTCoefficients::computeInverseP()`.

4.3.2 Solution for stratified samples

{Sstrapo}

We consider a stratified sample where both $\bar{v}_{\text{nucl}}(z)$ and $\mathbf{B}(\mathbf{r})$ are constant within one layer. The vertical wavefunction is then given by the spinor analog of ???. Within layer j , the wavefunction is

$$\underline{\Phi}_j(z) = e^{-i(z-z_j)\underline{p}_j} \underline{t}_j + e^{i(z-z_j)\underline{p}_j} \underline{r}_j \quad (4.48) \quad \{\{\text{EPhi j P}\}\}$$

with constant spinors $\underline{t}_j, \underline{r}_j$. The continuity conditions at the interface of layers a and $b := a + 1$ are analog to (2.35). In full analogy with (4.49), they can be resolved as

$$\begin{pmatrix} \underline{t}_a \\ \underline{r}_a \end{pmatrix} = \mathbb{M}_{ab} \begin{pmatrix} \underline{t}_b \\ \underline{r}_b \end{pmatrix}. \quad (4.49) \quad \{\{\text{EcMcP}\}\}$$

The double wavey underline shall indicate that the transfer matrix is now of dimension 4×4 . It is made of 2×2 blocks that consist of 2×2 matrices acting in spin space. As in ??, it can be written as a product

$$\mathbb{M}_{ab} = \mathbb{D}_a \mathbb{S}_{ab}. \quad (4.50) \quad \{\{\text{EMDSP}\}\}$$

The refraction matrix

$$\mathbb{S}_{ab} := \frac{1}{2} \begin{pmatrix} (1 + \underline{P}_{ab}) & (1 - \underline{P}_{ab}) \\ (1 - \underline{P}_{ab}) & (1 + \underline{P}_{ab}) \end{pmatrix} \quad (4.51) \quad \{\{\text{ESabP}\}\}$$

involves

$$\underline{P}_{ab} := \underline{p}_a^{-1} \underline{p}_b. \quad (4.52) \quad \{\{\text{ESabP}\}\}$$

The propagation matrix

$$\mathbb{D}_a := \begin{pmatrix} \underline{\delta}_a^{-1} & 0 \\ 0 & \underline{\delta}_a \end{pmatrix} \quad (4.53)$$

contains the phase-shift matrix

$$\underline{\delta}_j := e^{i \underline{d}_j \underline{p}_j} \quad (4.54) \quad \{\{\text{EdeltaP}\}\}$$

that generalizes ???.

4.3.3 Evaluation of the phase factors

{Sphase}

To make our implementation³ transparent, let us explain the evaluation of the phase-shift matrix (4.54) in some detail. The matrix $\mathbf{e}_{\mathbf{B}}\underline{\underline{\sigma}}$ has the eigenvalues ± 1 and the normalized eigenvectors

$$\underline{v}_+ = \frac{1}{\sqrt{2(1+e_z)}} \begin{pmatrix} 1+e_z \\ e_x + ie_y \end{pmatrix}, \quad \underline{v}_- = \frac{1}{\sqrt{2(1+e_z)}} \begin{pmatrix} -e_x + ie_y \\ 1+e_z \end{pmatrix}. \quad (4.55) \quad \{\{\mathbf{Ev1v2}\}\}$$

For readability, we have omitted the subscript \mathbf{B} from the components of $\mathbf{e}_{\mathbf{B}}$. The matrix \underline{p} has the eigenvalues λ_{\pm} , and the same eigenvectors (4.55) as $\mathbf{e}_{\mathbf{B}}\underline{\underline{\sigma}}$. We introduce the eigenvector matrix

$$\underline{Q} := (\underline{v}_+, \underline{v}_-). \quad (4.56) \quad \{\mathbf{Ev1v2}\}$$

Then \underline{p} has the eigenvalue decomposition

$$\underline{p} = \underline{Q} \begin{pmatrix} \lambda_+ & 0 \\ 0 & \lambda_- \end{pmatrix} \underline{Q}^\dagger, \quad (4.57)$$

and the phase-shift matrix (4.54) can be written

$$\underline{\delta} = \underline{Q} \begin{pmatrix} e^{id\lambda_+} & 0 \\ 0 & e^{id\lambda_-} \end{pmatrix} \underline{Q}^\dagger. \quad (4.58) \quad \{\{\mathbf{EdP2}\}\}$$

In the case $\mathbf{B} = 0$, we have $\lambda_+ = \lambda_-$, which has for consequence that (4.58) holds for whatever direction vector $\mathbf{e}_{\mathbf{B}}$; the simplest choice is $\mathbf{e}_{\mathbf{B}}(B=0) := \hat{\mathbf{z}}$ so that $\underline{Q} = \underline{1}$.

4.3.4 The split boundary problem

{SsplitbouP}

A numerically stable recursive solution of the split boundary problem for polarized radiation has been proposed in [15], and summarized in notation closer to ours in [16]. Their argument can be further simplified as follows.

SCALAR CASE:

We consider layers $a, b := a+1, \nu$. The transfer matrix (2.46) obeys the recursion

$$M_{a\nu} = M_{ab} M_{b\nu}. \quad (4.59) \quad \{\mathbf{EdP2}\}$$

With the conversion functions (2.48) and (2.49), we can derive a recursion for W :

$$W_{a\nu} = \mathcal{W}(M_{ab} \mathcal{M}(W_{b\nu})). \quad (4.60) \quad \{\{\mathbf{EWrecu}\}\}$$

The per-layer transfer matrices M_{ab} are given; the $W_{a\nu}$ shall be determined for a from $\nu-1$ to 0.

³In `MatrixRTCoefficients::computeDeltaMatrix`

Once we have $W_{0\nu}$, we can use

$$\begin{pmatrix} t_\nu \\ r_0 \end{pmatrix} = W_{0\nu} \begin{pmatrix} 1 \\ 0 \end{pmatrix} \quad (4.61) \quad \{\{\text{Ert_backward}\}\}$$

to compute the reflected amplitude r_0 in the top (air/vacuum) layer. This backward computation must then be followed by a forward computation of

$$\begin{pmatrix} t_a \\ r_a \end{pmatrix} = M_{0a}^{-1} \begin{pmatrix} 1 \\ r_0 \end{pmatrix}. \quad (4.62) \quad \{\{\text{Ert_forward}\}\}$$

THE FOLLOWING WAS OUTCOMMENTED:

However, determining the $W_{a\nu}$ is not a goal in itself; we shall only evaluate them insofar as needed for computing. Ultimately, we want to apply (4.63) to layers $i = 0$, $f = \nu$, with $r_\nu = 0$. Therefore, we only need to derive the tt and rt components of $W_{0\nu}$, whereas the tr and rr components are irrelevant. It turns out that this also holds for the inner terms of the recursion (4.60): we only need the tt and rt components of the intermediate W_{0a} .

NOW THE POLARIZED CASE

THE FOLLOWING WAS OUTCOMMENTED:

The homogeneous linear equation (4.49) can be reorganized as

$$\begin{pmatrix} t_f \\ r_i \end{pmatrix} = \mathbb{W}_{if} \begin{pmatrix} t_i \\ r_f \end{pmatrix} \quad (4.63) \quad \{\{\text{EcWcP}\}\}$$

for whatever layers j, k . Following [16], we write matrix components as

$$\mathbb{W} =: \begin{pmatrix} \underline{\underline{W}}^{tt} & \underline{\underline{W}}^{tr} \\ \underline{\underline{W}}^{rt} & \underline{\underline{W}}^{rr} \end{pmatrix}, \quad (4.64) \quad \{\{\text{EcWcP}\}\}$$

and similarly for matrix \mathbb{M} of (4.49). Combining (4.49) and (4.63), we can express \mathbb{W} as function of \mathbb{M} ,

$$\mathbb{W}(\mathbb{M}) = \begin{pmatrix} \underline{\underline{M}}^{tt-1} & \underline{\underline{M}}^{tt-1} \underline{\underline{M}}^{tr} \\ \underline{\underline{M}}^{rt} \underline{\underline{M}}^{tt-1} & (\underline{\underline{M}}^{rr} - \underline{\underline{M}}^{rt} \underline{\underline{M}}^{tt-1} \underline{\underline{M}}^{tr}) \end{pmatrix}, \quad (4.65) \quad \{\{\text{EM2Wpol}\}\}$$

and conversely, \mathbb{M} as function of \mathbb{W}

$$\mathbb{M}(\mathbb{W}) = ?? \quad (4.66) \quad \{\{\text{EW2Mpol}\}\}$$

Now consider layers $0, a, b := a + 1$. The transfer matrix obeys the recursion

$$\mathbb{M}_{0b} = \mathbb{M}_{0a} \mathbb{M}_{ab}. \quad (4.67) \quad \{\{\text{EW2Mpol}\}\}$$

With the conversions (4.65) and (4.66), we can derive a recursion for \mathbb{W} :

$$\mathbb{W}_{0b} = \mathbb{W}(\mathbb{M}(\mathbb{W}_{0a}) \mathbb{M}_{ab}). \quad (4.68) \quad \{\{\text{EWrecupo}\}\}$$

Ultimately, we want to apply (4.63) to layers $i = 0$, $f = \nu$, with $r_\nu = 0$. Therefore, we only need to derive the tt and rt components of $W_{0\nu}$, whereas the tr and rr components are irrelevant. It turns out that this also holds for the inner terms of the recursion (4.68): we only need the tt and rt components of the intermediate W_{0a} .

4.4 From old document “PolarizedImplementation”

4.4.1 Transfer Matrix

For a more detailed description of polarized reflectometry, we refer to the document *Summary Theory of Reflectivity* in theory/reflectivity.pdf.

The amplitudes are stored in four-component vectors that are written as $\begin{pmatrix} t_m, r_m \end{pmatrix}^T$. Both of these entries represent again a two-component spinor that describes the polarization state of the transmitted and reflected components.

Throughout our implementation, we apply the following representation of the polarized transfer matrix:

$$\begin{pmatrix} \underline{t}_a \\ \underline{r}_a \end{pmatrix} = \underbrace{\frac{1}{2} \begin{pmatrix} \delta_a^{-1} & 0 \\ 0 & \delta_a \end{pmatrix} \begin{pmatrix} 1 + p_a^{-1} p_b & 1 - p_a^{-1} p_b \\ 1 - p_a^{-1} p_b & 1 + p_a^{-1} p_b \end{pmatrix}}_{=: \mathbb{M}_\mathcal{D}} \begin{pmatrix} \underline{t}_b \\ \underline{r}_b \end{pmatrix} \quad (4.69) \quad \{\text{eq:interface_transfer_m}\}$$

$$= \frac{1}{2} \begin{pmatrix} \delta_a^{-1} & 0 \\ 0 & \delta_a \end{pmatrix} \begin{pmatrix} 1 + \underline{\underline{P}}_{ab} & 1 - \underline{\underline{P}}_{ab} \\ 1 - \underline{\underline{P}}_{ab} & 1 + \underline{\underline{P}}_{ab} \end{pmatrix} \begin{pmatrix} \underline{t}_b \\ \underline{r}_b \end{pmatrix}, \quad (4.70) \quad \{\text{eq:interface_transfer_ma}\}$$

with the phase factor

$$\underline{\underline{\delta}}_j := \exp i d_j p_j. \quad (4.71) \quad \{\text{eq:transfer_matrix_phas}\}$$

and the ratio of the moments $\underline{\underline{P}}_{ab} := \underline{\underline{p}}_a^{-1} \underline{\underline{p}}_b$, both of which are 2×2 matrices in the polarized case. This representation is consistent with the formulation in [56] and [57], where the transfer matrix representation is derived from the chosen ansatz for the wave functions. See theory/reflectivity.pdf for a derivation.

The transfer matrix $\mathbb{M}_\mathcal{D}$ for interface a is a product of two submatrices $\mathbb{M}_\mathcal{D} = \mathbb{D}_\mathcal{D} \mathbb{S}_\mathcal{D}$. $\mathbb{D}_\mathcal{D}$ propagates the amplitudes from the bottom of a layer of constant material to its top and the matrix $\mathbb{S}_\mathcal{D}$ describes the interface between layers a and $b = a + 1$.

The amplitudes on top of the multilayer stack can then be computed by

$$\begin{pmatrix} \underline{t}_0 \\ \underline{r}_0 \end{pmatrix} = \prod_{a=0}^{N-1} \mathbb{M}_\mathcal{D} \cdot \begin{pmatrix} \underline{t}_N \\ \underline{r}_N \end{pmatrix}, \quad (4.72) \quad \{\text{eq:total_transfer_matri}\}$$

where \underline{t}_N and \underline{r}_N are two-component spinors that contain the amplitudes at the bottom of the sample

4.4.2 Intensity Analysis

`\{sec:intensity_analysis\}`

The wave function in the ambient material is given by

$$\underline{\Phi}_0(z) = \underbrace{\exp i \underline{\underline{p}}_0 \underline{t}_0}_{\underline{\Phi}_i(z)} + \underbrace{\exp -i \underline{\underline{p}}_0 \underline{r}_0}_{\underline{\Phi}_r(z)}. \quad (4.73) \quad \{\text{eq:total_transfer_matrix}\}$$

Here $\underline{\Phi}_i$ is the incoming wave in a given polarization state \underline{t}_0 and $\underline{\Phi}_r$ is the reflected wave. The intensity measured on a detector is without polarization analysis given by

$$I_R = |\underline{\Phi}_r|^2 = \langle \underline{\Phi}_r | \underline{\Phi}_r \rangle \quad (4.74) \quad \{\text{eq:intensity_no_polariz}\}$$

This would allow for the direct computation of the reflected intensity if \underline{t}_0 would describe the incoming polarization state. In case of an arbitrary but pure state of the incoming beam, the reflected wave can be described by a reflection matrix

$$\underline{\Phi}_r(z) = \underline{\mathcal{R}} \underline{\Phi}_i(z), \quad (4.75) \quad \{\text{eq:intensity_no_polariza}\}$$

where $\underline{\mathcal{R}}$ is a 2×2 matrix:

$$\underline{\mathcal{R}} = \begin{pmatrix} r_{++} & r_{-+} \\ r_{+-} & r_{--} \end{pmatrix} \quad (4.76)$$

with its non-diagonal elements contributing to spin-flip reflections. If we consider the intensities right at the topmost interface of the sample at $z = z_0 = 0$, the phase factors drop out and we find the relation

$$\underline{r}_0 = \underline{\mathcal{R}} \underline{t}_0. \quad (4.77) \quad \{\text{eq:R-matrix}\}$$

Therefore, as soon as $\underline{\mathcal{R}}$ is known, it is trivial to perform a calculation for any desired incoming polarization state. It is clear that (4.77) is a system of two equations with four unknown variables. Hence if two pairs of incoming and reflected waves $\underline{t}_0, \underline{r}_0$ and $\underline{t}'_0, \underline{r}'_0$ are known, the reflection matrix can be determined (if they are linearly independent). Writing these four equations as a matrix

$$(\underline{r}_0, \underline{r}'_0) = \underline{\mathcal{R}} (\underline{t}_0, \underline{t}'_0), \quad (4.78) \quad \{\text{eq:R-matrix2}\}$$

one can see that the inversion of this equation becomes trivial if the two incoming waves are chosen such that they are in a $+$ and $-$ polarization state. If they are chosen differently, inverting equation (4.78) corresponds to the rotation of the incoming polarization vectors such that they become pure $+$ and $-$ waves.

If we perform polarization analysis, the analyzer will only pass a wave in the $\underline{\Phi}_f$ polarization state. Hence the reflected wave needs to be projected onto this state to obtain the measured intensity

$$I_R = \left| \langle \underline{\Phi}_f | \underline{\mathcal{R}} | \underline{\Phi}_i \rangle \right|^2 = \langle \underline{\Phi}_f | \underline{\mathcal{R}} | \underline{\Phi}_i \rangle \cdot \langle \underline{\Phi}_i | \underline{\mathcal{R}}^\dagger | \underline{\Phi}_f \rangle. \quad (4.79) \quad \{\text{eq:intensity_polarizati}\}$$

Following [58], we introduce the density matrix \underline{f}_p (polarizer) for an arbitrary mixed state of incoming beam and, correspondingly, \underline{f}_a (analyzer) for an arbitrary mixed state passed through a polarization analyzer:

$$\underline{f}_p = \frac{1}{2} (\underline{1} + \underline{\sigma} \cdot \underline{p}) \quad \underline{f}_a = \frac{1}{2} (\underline{1} + \underline{\sigma} \cdot \underline{a}). \quad (4.80) \quad \{\text{eq:density_operators}\}$$

The beam polarization as well as analyzer direction and efficiency are described by the Bloch vectors $\mathbf{p}, \mathbf{a} \in \mathbb{R}^3$. $|\mathbf{p}| = 1$ corresponds to some pure state of beam polarization, while $|\mathbf{p}| < 1$ is for a state mixture (partial polarization). The same holds for non-perfect analyzers, where we call $|\mathbf{p}|$ the efficiency.⁴

In order to compute the reflection coefficient for a mixed-state beam, equation (4.79) needs to be rewritten in the density matrix formalism

$$\langle \underline{\Phi}_i | \underline{\mathcal{R}}^\dagger | \Psi_f \rangle \cdot \langle \underline{\Phi}_f | \underline{\mathcal{R}} | \underline{\Phi}_i \rangle = \text{Tr} \left(|\underline{\Phi}_i\rangle \langle \underline{\Phi}_i| \underline{\mathcal{R}}^\dagger |\underline{\Phi}_f\rangle \langle \underline{\Phi}_f| \underline{\mathcal{R}} \right). \quad (4.81) \quad \{\text{eq:intensity_trace}\}$$

Here Tr denotes trace operation. $|\underline{\Phi}_f\rangle \langle \underline{\Phi}_f|$ and $|\underline{\Phi}_i\rangle \langle \underline{\Phi}_i|$ are respective outer products for the $\underline{\Phi}_f$ and $\underline{\Phi}_i$ pure states and coincide with the corresponding density matrices. To generalize expression (4.81) to mixed states of the incoming beam and polarization analyzer, one has to replace the explicit outer products with the density matrices $\underline{f}_p, \underline{f}_a$ that describe the polarizer and analyzer as defined in (4.80). This will automatically take into account the averaging over all possible initial and final pure states of the system. Therefore, the final expression for I_R reads

$$I_R = \text{Tr} \left(\underline{f}_p \underline{\mathcal{R}}^\dagger \underline{f}_a \underline{\mathcal{R}} \right). \quad (4.82) \quad \{\text{eq:32}\}$$

This expression should work for both a perfect and imperfect polarizer and analyzer. It also seems to be consistent with Wildes [59, 60], this paper was recommended as standard reference on this topic by Artur.

It needs to be noted that the limit $|\underline{a}| = 0$ does not correspond to no polarization analysis (i.e. a very common experiment without polarization analysis). Instead, if no polarization analysis is performed, writing (4.74) in the density matrix formalism yields

$$I_R = |\underline{\Phi}_r|^2 = \langle \underline{\Phi}_i | \underline{\mathcal{R}}^\dagger \underline{\mathcal{R}} | \underline{\Phi}_i \rangle = \text{Tr} \left(\underline{f}_p \underline{\mathcal{R}}^\dagger \underline{\mathcal{R}} \right), \quad (4.83) \quad \{\text{eq:32}\}$$

which corresponds to $\underline{f}_a = \underline{1}$.

TODO: can we show the equivalence between the Wildes approach and our density matrix formulas?

4.4.3 Numerically Stable Implementation

{sec:implementation}

We combine the amplitude vectors for $+$ and $-$ polarization into a single matrix of dimension 4×2

$$\begin{pmatrix} \underline{T}_j \\ \underline{R}_j \end{pmatrix} = \begin{pmatrix} \underline{t}_j^+ & \underline{t}_j^- \\ \underline{r}_j^+ & \underline{r}_j^- \end{pmatrix}, \quad \underline{T}_j = (\underline{t}_j^+, \underline{t}_j^-), \quad \underline{R}_j = (\underline{r}_j^+, \underline{r}_j^-), \quad (4.84)$$

⁴In PolarizedSpecular, Sec. 5.1, Dmitry claims this treatment of a non-perfect analyzer is not possible and suggests a different treatment. However i (rb) think that his argument is not correct.

where the submatrices $\underline{\underline{T}}_j$ and $\underline{\underline{R}}_j$ are of dimension 2×2 . The recursion equation (4.69) can then be written simultaneously for both polarization states as

$$\begin{pmatrix} \underline{\underline{T}}_a \\ \underline{\underline{R}}_a \end{pmatrix} = \frac{1}{2} \begin{pmatrix} \underline{\underline{\delta}}_a^{-1} & 0 \\ 0 & \underline{\underline{\delta}}_a \end{pmatrix} \begin{pmatrix} 1 + \underline{\underline{P}}_{ab} & 1 - \underline{\underline{P}}_{ab} \\ 1 - \underline{\underline{P}}_{ab} & 1 + \underline{\underline{P}}_{ab} \end{pmatrix} \begin{pmatrix} \underline{\underline{T}}_b \\ \underline{\underline{R}}_b \end{pmatrix}. \quad (4.85)$$

Explicitly performing this multiplication yields two matrix recursion equations

$$\underline{\underline{T}}_a = \frac{1}{2} \underline{\underline{\delta}}_a^{-1} \left(\left(1 + \underline{\underline{P}}_{ab} \right) \underline{\underline{T}}_b + \left(1 - \underline{\underline{P}}_{ab} \right) \underline{\underline{R}}_b \right) \quad (4.86)$$

$$\underline{\underline{R}}_a = \frac{1}{2} \underline{\underline{\delta}}_a \left(\left(1 - \underline{\underline{P}}_{ab} \right) \underline{\underline{T}}_b + \left(1 + \underline{\underline{P}}_{ab} \right) \underline{\underline{R}}_b \right) \quad (4.87)$$

After every step of the iteration (4.72), we want to rotate and normalize the polarization, such that we obtain the bottom boundary condition $\underline{\underline{T}}_a = \underline{\underline{1}}$. For this purpose, we define the rotation matrix $\underline{\underline{S}}$ as

$$\underline{\underline{T}}'_a = \underline{\underline{T}}_a \cdot \underline{\underline{S}}_a = \underline{\underline{1}}, \quad (4.88)$$

and it must also be applied to rotate the reflected components as well ⁵

$$\underline{\underline{R}}'_a = \underline{\underline{R}}_a \cdot \underline{\underline{S}}_a. \quad (4.89)$$

Consequently, the recursion equations reduce to the primed version

{eq:primed_recursion}

$$\underline{\underline{T}}'_a = \underline{\underline{1}} \quad (4.90a)$$

$$\underline{\underline{S}}_a^{-1} = \frac{1}{2} \underline{\underline{\delta}}_a^{-1} \left(\left(1 + \underline{\underline{P}}_{ab} \right) + \left(1 - \underline{\underline{P}}_{ab} \right) \underline{\underline{R}}'_b \right) =: \underline{\underline{\delta}}_a^{-1} \cdot \underline{\underline{\tilde{S}}}_a^{-1} \quad (4.90b)$$

$$\underline{\underline{R}}'_a = \frac{1}{2} \underline{\underline{\delta}}_a \left(\left(1 - \underline{\underline{P}}_{ab} \right) + \left(1 + \underline{\underline{P}}_{ab} \right) \underline{\underline{R}}'_b \right) \cdot \underline{\underline{S}}_a. \quad (4.90c)$$

This process requires the inverse of $\underline{\underline{S}}_a^{-1}$, which is easy to obtain

$$\underline{\underline{S}}_a = \frac{1}{\det \underline{\underline{\tilde{S}}}_a^{-1}} \begin{pmatrix} \left(\underline{\underline{\tilde{S}}}_a^{-1} \right)_{1,1} & - \left(\underline{\underline{\tilde{S}}}_a^{-1} \right)_{1,0} \\ - \left(\underline{\underline{\tilde{S}}}_a^{-1} \right)_{0,1} & \left(\underline{\underline{\tilde{S}}}_a^{-1} \right)_{0,0} \end{pmatrix} \underline{\underline{\delta}}_a, \quad (4.91)$$

and since it does not contain the inverse δ^{-1} -matrix anymore can be evaluated numerically stable.

⁵What happens here is a rotation of the wave function written as a superposition $\underline{\underline{\Phi}}'_a{}^\pm = a^\pm \underline{\underline{\Phi}}_a{}^+ + b^\pm \underline{\underline{\Phi}}_a{}^-$. This is just written as a single matrix equation and from this it is obvious that the same matrix must be applied to both $\underline{\underline{T}}_a$ and $\underline{\underline{R}}_a$.

For the computation of reflectivity alone, we would be done at this point, however, for perturbation theory, we still need the amplitudes within the layer stack. Therefore, all rotations of the polarization need to be forward-propagated according to

$$\underline{\underline{T}}_a = \prod_{i=m-1}^0 \underline{\underline{S}}_i \quad (4.92)$$

$$\underline{\underline{R}}_a = \underline{\underline{R}}'_a \cdot \prod_{i=m-1}^0 \underline{\underline{S}}_i \quad (4.93)$$

$$\text{for } a \geq 1, \text{ where } \prod_{i=m-1}^0 \underline{\underline{S}}_i = \underline{\underline{S}}_{a-1} \underline{\underline{S}}_{a-2} \cdots \underline{\underline{S}}_0 \quad (4.94)$$

The proof of these relations can be done as follows. In order to obtain the correct amplitudes in each layer, after every step of the recursion (4.90) the applied rotation needs to be propagated down through the bottom of the stack according to

$$\text{for } m = N - 1 \dots 0 \quad \text{outer iteration from bottom to top} \quad (4.95)$$

$$\underline{\underline{T}}'_m = \underline{\underline{1}} \quad (4.96)$$

$$\underline{\underline{R}}'_m = \underline{\underline{R}}_m \cdot \underline{\underline{S}}_m \quad (4.97)$$

$$\text{for } i = m + 1 \dots N \quad (4.98)$$

$$\underline{\underline{T}}_i = \underline{\underline{T}}_i \cdot \underline{\underline{S}}_m \quad (4.99)$$

$$\underline{\underline{R}}_i = \underline{\underline{R}}_i \cdot \underline{\underline{S}}_m \quad (4.100)$$

Remark The defined $\underline{\underline{R}}'_m$ is equal to the $\underline{\underline{X}}_m$ in the Parratt formalism and equation (4.90)c is almost identical to the usual recursion in $\underline{\underline{X}}_m$ [56, 57], apart from the treatment of the phase factor. The second recursion equation in [56, 57] that yields the amplitudes is replaced by storing the intermediate $\underline{\underline{S}}_m$.

`Compute::SpecularMagnetic::topLayerR` contains a lightweight implementation that does not store coefficients of intermediate layers and hence only computes the coefficient of the top layer and hence reflection. This was introduced in order to speed up pure reflectometry computations. This is similarly implemented for the scalar implementation.

4.4.4 Evaluation of the Matrices $\underline{\underline{p}}$ and $\underline{\underline{p}}^{-1}$

Using the well-known representation of the Pauli matrices, the matrix $\underline{\underline{p}}_a$ is explicitly given by

$$\underline{\underline{p}} = \frac{1}{2} (\alpha + \beta \mathbf{e}_B \underline{\underline{\sigma}}) \quad (4.101)$$

$$= \frac{1}{2} \begin{pmatrix} \alpha + \beta e_z & \beta (e_x - i e_y) \\ \beta (e_x + i e_y) & \alpha - \beta e_z \end{pmatrix} \quad (4.102)$$

with

$$\alpha := \lambda_+ + \lambda_- , \quad \beta := \lambda_+ - \lambda_- . \quad (4.103)$$

λ_+ and λ_- are the eigenvalues of the operator \underline{p} . The inverse is given by

$$\underline{p}^{-1} = \frac{2}{\alpha^2 - \beta^2} \begin{pmatrix} \alpha - \beta e_z & -\beta(e_x - ie_y) \\ -\beta(e_x + ie_y) & \alpha + \beta e_z \end{pmatrix} . \quad (4.104)$$

4.4.5 Evaluation of the Phase Factors

We have

$$\exp i \underline{p} d = \exp i \frac{d}{2} \alpha \cdot \exp i \frac{d}{2} \beta \mathbf{e}_{\mathbf{B}} \underline{\sigma} , \quad (4.105)$$

where d is the thickness of the current layer. For convenience, we define

$$\alpha' = d\alpha/2 , \quad (4.106)$$

$$\beta' = d\beta/2 . \quad (4.107)$$

With this abbreviation we can write

$$\exp i \underline{p} d = \exp i \alpha' \cdot \exp i \beta' \mathbf{e}_{\mathbf{B}} \underline{\sigma} . \quad (4.108)$$

Evaluation of the first part is easy because it is diagonal (which is also the reason that the multiplication of the two exponential functions works). The matrix in the second factor has the eigenvalues $\pm\beta'$ and its eigenvectors are given by

$$\underline{v}_1 = \frac{1}{\sqrt{2(1+e_z)}} \begin{pmatrix} e_z + 1 \\ ie_y + e_x \end{pmatrix} \quad \underline{v}_2 = \frac{1}{\sqrt{2(1+e_z)}} \begin{pmatrix} ie_y - e_x \\ e_z + 1 \end{pmatrix} , \quad (4.109) \quad \{\text{eq:transformation_matrix}\}$$

so that the eigenvalue decomposition of the matrix $\beta' \mathbf{e}_{\mathbf{B}} \underline{\sigma}$ is given by

$$\beta' \mathbf{e}_{\mathbf{B}} \underline{\sigma} = \underline{Q} \cdot \begin{pmatrix} +\beta' & 0 \\ 0 & -\beta' \end{pmatrix} \underline{Q}^\dagger \quad \underline{Q} = (\underline{v}_1, \underline{v}_2) . \quad (4.110)$$

Then we have

$$\exp i \underline{p} d = \exp i \alpha' \underline{Q} \cdot \begin{pmatrix} \exp +\beta' & \\ & \exp -\beta' \end{pmatrix} \cdot \underline{Q}^\dagger . \quad (4.111)$$

It needs to be stressed that this form strictly needs a normalized real vector $\mathbf{e}_{\mathbf{B}}$. Furthermore, this form is not very convenient for numerical evaluations since the exponential factor with $-\beta'$ turns very large and leads to an overflow. For this reason, the first diagonal exponential matrix can be multiplied inside to obtain

$$\exp i \underline{p} d = \underline{Q} \begin{pmatrix} \exp i d \lambda_+ & 0 \\ 0 & \exp i d \lambda_- \end{pmatrix} \underline{Q}^\dagger \quad (4.112)$$

The case $\mathbf{e}_{\mathbf{B}} = 0$ needs to be considered separately, then $\beta = 0$ and obviously

$$\exp i \underline{p} d = \exp i \alpha' \cdot \underline{1} \quad (4.113)$$

4.4.6 Roughness

For a detailed description of the implemented roughness models, we refer to the document *Refraction, reflection, and scattering from rough interfaces* in theory/Roughness.pdf.

4.4.6.1 Tanh Profile

As in the scalar implementation, the analytical tanh interface profile is implemented by replacing the Fresnel reflection and transmission coefficients in the transfer matrix

$$\underline{\underline{S}}_{ab} = \begin{pmatrix} 1 + \underline{\underline{P}}_{ab} & 1 - \underline{\underline{P}}_{ab} \\ 1 - \underline{\underline{P}}_{ab} & 1 + \underline{\underline{P}}_{ab} \end{pmatrix} \quad (4.114)$$

to incorporate the analytical solution of the Helmholtz equation via

$$\underline{\underline{S}}_{ab} = \begin{pmatrix} 1/\underline{\underline{\mathcal{R}}}_{ab} + \underline{\underline{P}}_{ab}\underline{\underline{\mathcal{R}}}_{ab} & 1/\underline{\underline{\mathcal{R}}}_{ab} - \underline{\underline{P}}_{ab}\underline{\underline{\mathcal{R}}}_{ab} \\ 1/\underline{\underline{\mathcal{R}}}_{ab} - \underline{\underline{P}}_{ab}\underline{\underline{\mathcal{R}}}_{ab} & 1/\underline{\underline{\mathcal{R}}}_{ab} + \underline{\underline{P}}_{ab}\underline{\underline{\mathcal{R}}}_{ab} \end{pmatrix}. \quad (4.115)$$

Here, the roughness correction factor $\underline{\underline{\mathcal{R}}}_{ab}$ is also a 2×2 matrix and is given by

$$\underline{\underline{\mathcal{R}}}_{ab} = \frac{\sqrt{\tanhc \left\{ (\pi/2)^{3/2} \underline{\underline{\sigma}}_a \underline{\underline{p}}_b \right\}}}{\sqrt{\tanhc \left\{ (\pi/2)^{3/2} \underline{\underline{\sigma}}_a \underline{\underline{p}}_a \right\}}} = \underline{\underline{\mathcal{R}}}_b \cdot \underline{\underline{\mathcal{R}}}_a^{-1} \quad (4.116)$$

This expression is evaluated via the eigenvalue decomposition

$$\underline{\underline{\mathcal{R}}}_b = \underline{\underline{Q}}_b \begin{pmatrix} \sqrt{\tanhc \left(\underline{\underline{\sigma}}'_a \lambda_+^b \right)} & 0 \\ 0 & \sqrt{\tanhc \left(\underline{\underline{\sigma}}'_a \lambda_-^b \right)} \end{pmatrix} \underline{\underline{Q}}_b^\dagger \quad (4.117) \quad \{\text{eq:roughness_tanh_eigen}\}$$

$$\underline{\underline{\mathcal{R}}}_a^{-1} = \underline{\underline{Q}}_a \begin{pmatrix} \frac{1}{\sqrt{\tanhc \left(\underline{\underline{\sigma}}'_a \lambda_+^a \right)}} & 0 \\ 0 & \frac{1}{\sqrt{\tanhc \left(\underline{\underline{\sigma}}'_a \lambda_-^a \right)}} \end{pmatrix} \underline{\underline{Q}}_a^\dagger, \quad (4.118) \quad \{\text{eq:roughness_tanh_eigen}\}$$

where we have defined $\underline{\underline{\sigma}}'_a = (\pi/2)^{3/2} \underline{\underline{\sigma}}_a$ and the transformation matrix $\underline{\underline{Q}}$ is the same as in equation (4.109).

The case of zero magnetic field $\vec{e}_b = 0$ needs to be treated separately again, in that case we have

$$\underline{\underline{\mathcal{R}}}_b = \begin{pmatrix} \sqrt{\tanh c \left(1/2 \underline{\underline{\sigma}}'_a \alpha_b \right)} & 0 \\ 0 & \sqrt{\tanh c \left(1/2 \underline{\underline{\sigma}}'_a \alpha_b \right)} \end{pmatrix} \quad (4.119)$$

$$\underline{\underline{\mathcal{R}}}_a^{-1} = \begin{pmatrix} \frac{1}{\sqrt{\tanh c \left(1/2 \underline{\underline{\sigma}}'_a \alpha_a \right)}} & 0 \\ 0 & \frac{1}{\sqrt{\tanh c \left(1/2 \underline{\underline{\sigma}}'_a \alpha_a \right)}} \end{pmatrix} \quad (4.120)$$

4.4.6.2 Névot-Croce

The interface transition part of the transfer matrix is replaced with the expression

$$\underline{\underline{S}}_{ab} = \frac{1}{2} \begin{pmatrix} (1 + \underline{\underline{P}}) \exp - \left(\underline{\underline{p}}_b - \underline{\underline{p}}_a \right)^2 \frac{\underline{\underline{\sigma}}_a^2}{2} & (1 - \underline{\underline{P}}) \exp - \left(\underline{\underline{p}}_b + \underline{\underline{p}}_a \right)^2 \frac{\underline{\underline{\sigma}}_a^2}{2} \\ (1 - \underline{\underline{P}}) \exp - \left(\underline{\underline{p}}_b + \underline{\underline{p}}_a \right)^2 \frac{\underline{\underline{\sigma}}_a^2}{2} & (1 + \underline{\underline{P}}) \exp - \left(\underline{\underline{p}}_b - \underline{\underline{p}}_a \right)^2 \frac{\underline{\underline{\sigma}}_a^2}{2} \end{pmatrix}, \quad (4.121) \quad \text{\texttt{\{eq:transfer_matrix_Giba}}}$$

that is the polarized equivalent of the scalar implementation. For brevity the indices on the $\underline{\underline{P}}_{ab}$ matrices are omitted in this section. In order to evaluate this matrix, we need to compute the exponential of a matrix of the form

$$\underline{\underline{P}}_{ab} = \left(\underline{\underline{p}}_b \pm \underline{\underline{p}}_a \right)^2. \quad (4.122)$$

This matrix can be rewritten as

$$\underline{\underline{P}}_{ab} = \underline{\underline{p}}_b \pm \underline{\underline{p}}_a \quad (4.123)$$

$$= \frac{1}{2} \left[\alpha_b \pm \alpha_a + \underline{\underline{\sigma}} \cdot \underbrace{\left(\beta_b \vec{b}_b \pm \beta_a \vec{b}_a \right)}_{:= \vec{b}'} \right]. \quad (4.124)$$

Now the vector \vec{b}' is a complex vector, that will be normalized according to

$$\vec{b}'' = \frac{\vec{b}'}{\vec{b}'^T \cdot \vec{b}'}, \quad (4.125)$$

and we have the new eigenvalue

$$\beta_{ab} = \vec{b}''^T \cdot \vec{b}'. \quad (4.126)$$

It must be noted, that this normalization is not based on the usual inner product with a complex conjugate, but really only the squared elements of the vector. This is due to the fact that the p -matrix is only squared and not conjugated. The vectors \vec{b}' and \vec{b}''

should carry a \pm , depending on which matrix is being evaluated, however, for clarity we drop this sign. Consequently, we can now write the resulting matrix

$$\underline{\underline{P}}_{ab} = \frac{1}{2} \left(\alpha_{ab} + \beta_{ab} \underline{\underline{\sigma}} \cdot \vec{b}'' \right), \quad (4.127)$$

with $\alpha_{ab} = \alpha_b \pm \alpha_a$. This expression can easily be squared

$$\underline{\underline{P}}_{ab}^2 = \frac{1}{4} \left(\alpha_{ab}^2 + \beta_{ab}^2 + 2\alpha_{ab}\beta_{ab} \underline{\underline{\sigma}} \cdot \vec{b}'' \right) \quad (4.128)$$

$$= \frac{1}{4} \left(\alpha''_{\underline{\underline{1}}} + \beta''_{\underline{\underline{\sigma}}} \cdot \vec{b}'' \right). \quad (4.129)$$

The exponential of this can now be computed using the well-known eigendecomposition of the second term. The eigenvalues are now $\pm\beta''$ and the corresponding eigenvectors are given by

$$\underline{v}_1 = \frac{1}{\sqrt{2(b''_z + 1)}} \begin{pmatrix} 1 + b''_z \\ b''_x + ib''_y \end{pmatrix} \quad \underline{v}_2 = \frac{1}{\sqrt{2(1 - b''_z)}} \begin{pmatrix} b''_z - 1 \\ b''_x + ib''_y \end{pmatrix}, \quad (4.130)$$

such that we have the usual eigenvalue equation $\underline{\underline{Q}}v_n = \beta''v_n$ with $\underline{\underline{Q}} = (\underline{v}_1, \underline{v}_2)$. The inverse $\underline{\underline{Q}}^{-1}$ is given by

$$\underline{\underline{Q}}^{-1} = \begin{pmatrix} v'_1{}^T \\ v'_2{}^T \end{pmatrix}, \quad (4.131)$$

where

$$\underline{v}'_1 = \frac{1}{\sqrt{2(b''_z + 1)}} \begin{pmatrix} 1 + b''_z \\ b''_x - ib''_y \end{pmatrix} \quad \underline{v}'_2 = \frac{1}{\sqrt{2(1 - b''_z)}} \begin{pmatrix} b''_z - 1 \\ b''_x - ib''_y \end{pmatrix}. \quad (4.132)$$

Putting this all together, we obtain for $\vec{b}'' \neq 0$

$$\exp - \left(\underline{\underline{p}}_b - \underline{\underline{p}}_a \right)^2 \underline{\underline{\sigma}}_b^2 / 2 = \begin{pmatrix} \exp \alpha'' & 0 \\ 0 & \exp \alpha'' \end{pmatrix} \cdot \underline{\underline{Q}} \cdot \begin{pmatrix} \exp \beta'' & 0 \\ 0 & \exp -\beta'' \end{pmatrix} \underline{\underline{Q}}^{-1} \quad (4.133)$$

and for $\vec{b}'' = 0$

$$\exp - \left(\underline{\underline{p}}_b - \underline{\underline{p}}_a \right)^2 \sigma_b^2 / 2 = \begin{pmatrix} \exp \alpha'' & 0 \\ 0 & \exp \alpha'' \end{pmatrix}. \quad (4.134)$$

For brevity, the factor $\underline{\underline{\sigma}}_b^2 / 2$ was neglected in α'' and β'' .

4.4.7 Reflection Matrix and Boundary Conditions

In the current formalism, the reflection operator is directly computed by the implemented iterative method and given by $\underline{\underline{R}}_0$. In order to start the backwards iteration described in Section 4.4.3, one needs to impose the bottom boundary condition of no reflected wave, i.e. $\underline{\underline{R}}_N = \underline{\underline{0}}$. Furthermore, the iteration starts with pure polarization states, i.e. $\underline{\underline{T}}_N = \underline{\underline{1}}$, that is subsequently rotated to the final transmitted polarization state, by applying the top boundary condition $\underline{\underline{T}}_0 = \underline{\underline{1}}$.

4.4.8 Amplitudes for DWBA Computations

The DWBA computations require all four amplitudes that belong to the 4 waves traveling with different wave vectors separately. This requires the decomposition of

$$\underline{\Phi}_j(z) = \exp i \underline{\underline{p}}_a(z - z_{j-1}) \underline{t}_j + \exp -i \underline{\underline{p}}_a(z - z_{j-1}) \underline{r}_j, \quad (4.135)$$

into its eigenmodes. In order to achieve this, we again apply the eigenvalue decomposition of $\underline{\underline{p}}_a$, as it is also used in (4.117), where the transformation matrix is given by (4.109) and the eigenvalues are of course λ_+ and λ_- and we have

$$\exp i \underline{\underline{p}}_j z = \underline{\underline{Q}} \cdot \exp i \Lambda z \cdot \underline{\underline{Q}}^\dagger \quad (4.136)$$

$$= \underline{\underline{Q}} \cdot \begin{pmatrix} \exp i \lambda_+ z & 0 \\ 0 & 0 \end{pmatrix} \cdot \underline{\underline{Q}}^\dagger + \underline{\underline{Q}} \cdot \begin{pmatrix} 0 & 0 \\ 0 & \exp i \lambda_- z \end{pmatrix} \cdot \underline{\underline{Q}}^\dagger \quad (4.137)$$

$$= \exp i \lambda_+ z \underline{\underline{Q}} \cdot \begin{pmatrix} 1 & 0 \\ 0 & 0 \end{pmatrix} \cdot \underline{\underline{Q}}^\dagger + \exp i \lambda_- z \underline{\underline{Q}} \cdot \begin{pmatrix} 0 & 0 \\ 0 & 1 \end{pmatrix} \cdot \underline{\underline{Q}}^\dagger. \quad (4.138)$$

This decomposition is valid unless the magnetic field vanishes. In the latter case, we have

$$\exp i \underline{\underline{p}}_a z = \exp i \lambda_+ z \cdot \begin{pmatrix} 1 & 0 \\ 0 & 0 \end{pmatrix} + \exp i \lambda_- z \cdot \begin{pmatrix} 0 & 0 \\ 0 & 1 \end{pmatrix}. \quad (4.139)$$

The resulting matrix can be written as a sum of two matrices

$$\exp i \underline{\underline{p}}_a z = \exp i \lambda_+ z \underline{\underline{T}}_2 + \exp i \lambda_- z \underline{\underline{T}}_1, \quad (4.140)$$

and the needed amplitudes are then given by

$$\underline{\underline{T}}_1^+ = \underline{\underline{T}}_1 \cdot \underline{t} \quad \underline{\underline{R}}_1^+ = \underline{\underline{T}}_1 \cdot \underline{r} \quad \dots \quad (4.141)$$

The matrices $\underline{\underline{T}}_1$ and $\underline{\underline{T}}_2$ are computed via `MatrixRTCoefficients::T1Matrix` and `MatrixRTCoefficients::T2Matrix`.

These vector amplitudes $\underline{\underline{T}}_1^+$ etc. are computed in `MatrixRTCoefficients::T1plus` etc.

4.4.9 Limiting Case $\kappa \rightarrow 0$

This case is implemented in the same way as for the scalar case, that is described in Sec. 2.2.2 of the BornAgain manual version 1.7.2. For clarity, we briefly summarize the treatment here.

- One single layer: This is a trivial case, nothing needs to be calculated here as the outgoing wave is equal to the incoming one. As a consequence, it means that we have $\underline{\underline{T}}_0 = \underline{\underline{1}}$ and $\underline{\underline{R}}_0 = 0$
- More than one layer: In that case the limit $\kappa \rightarrow 0$ is well defined. For $\kappa = 0$, we have $\underline{\underline{R}}_0 = -\underline{\underline{T}}_0 = -\underline{\underline{1}}$ and $\underline{\underline{T}}_j = \underline{\underline{R}}_j = 0$ for $j > 0$.
- $\kappa = 0$ in intermediate layer: This case is not treated separately but automatically covered by the solution also present for scalar computations. In `KzComputation::checkForUnderflow` a tiny imaginary part is added if the resulting value for κ^2 is getting very small.

For a single layer, the correct computation of these conditions is checked in `SpecularMagneticTest::test_degenera`

4.4.10 Test Suite

The scalar amplitudes allow the computation of vector amplitudes according to

$$\begin{array}{cccc} \underline{\underline{T}}_1^+ = 0 & \underline{\underline{T}}_2^+ = \begin{pmatrix} t \\ 0 \end{pmatrix} & \underline{\underline{T}}_1^- = \begin{pmatrix} 0 \\ t \end{pmatrix} & \underline{\underline{T}}_2^- = 0 \\ \underline{\underline{R}}_1^+ = 0 & \underline{\underline{R}}_2^+ = \begin{pmatrix} r \\ 0 \end{pmatrix} & \underline{\underline{R}}_1^- = \begin{pmatrix} 0 \\ r \end{pmatrix} & \underline{\underline{R}}_2^- = 0 \end{array}$$

These relations allow to compare the amplitudes from a scalar computation to a polarized result, in case there is no magnetization present. For two layers, consistency between the scalar and polarized computation is checked in `SpecularMagneticTest::testZeroField`

4.4.11 Magnetic Field in BornAgain

The z-component is afaik currently explicitly set conserved.

Imo this is bit funny, as Dmitry also remarked in [Issue 2417](#)

4.4.11.1 Magnetic field in the fronting medium

As previously described in [5], it is reasonable to assume that the incoming beam penetrates the fronting medium of the sample assembly from a side. This results in k_z being preserved even when there is a non-zero magnetic field in the fronting medium. To account for that in the calculations, one needs to replace k_{0z}^2 with $k_{0z}^2 + 4\pi\check{\rho}_{front}$ in equation ??, with $\check{\rho}_{front}$ being the SLD matrix for the fronting medium. It is also equivalent to subtracting the magnetic field of the fronting medium, \mathbf{B}_{front} , from the magnetic field of each layer, thus amending $\check{\rho}_M$:

$$\check{\rho}'_M = -\frac{m}{2\pi\hbar^2}\check{\boldsymbol{\mu}}(\mathbf{B} - \mathbf{B}_{front}).$$

This amendment also concerns the nuclear (non-magnetic) scattering length density:

$$\rho'_n = \rho_n - \rho_{n,front},$$

where $\rho_{n,front}$ is the nuclear SLD of the fronting medium.

TODO: Check this in the code

Further in the text we will omit the primes and handling of the fronting medium's properties, however, implying that both magnetic fields and nuclear SLDs are amended in the way mentioned above.

4.4.11.2 Magnetic field z -component conservation

In the framework of the problem, the sample is assumed to be infinite along the x and y axes, all parameters being constant inside each layer. This is equivalent to the requirement of translational invariance along these axes. On the other hand, magnetic field is known to be divergence-free,

$$\nabla \cdot \mathbf{B} = 0.$$

Both of these conditions result in the z -component of the magnetic field (that is, the component normal to the sample surface), B_z , being preserved in the whole sample and fronting medium:

$$\frac{\partial B_z}{\partial z} \equiv 0.$$

4.4.12 Further (Potential) Problems

- $k_0^2 = 4\pi\rho^N$
- Many layers leading to infinity
- Zero k -vector inside sample at critical angle? Probably not an issue, resolved due to checkforunderflow in `kzcomputation.cpp`
- Branch cut from complex square-root?

5 Instrument simulation

5.1 Incoming beam and resolution

{SInstr}

{SBeam}

to be written ...



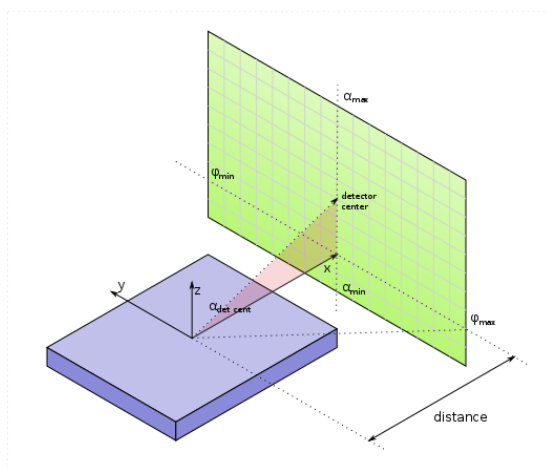


Figure 5.1: Experimental geometry with a two-dimensional pixel detector.

{FexpGeom}

5.2 Detector images

{SdetImg}

To conclude this chapter on the foundations of small-angle scattering, we shall derive the geometric factors that allow us to convert differential cross sections into detector counts. We shall also discuss how to present data on a physically meaningful scale.

5.2.1 Pixel coordinates, scattering angles, and \mathbf{q} components

We assume that scattered radiation is detected in a flat, two-dimensional detector that generates histograms on a rectangular grid, consisting of $n \cdot m$ pixels of constant width and height, as sketched in Fig. 5.1. This figure also shows the coordinate system according to unanimous GISAS convention, with z normal to the sample plane, and with the incident beam in the xz plane. The origin is at the center of the sample surface. We suppose that the detector is mounted perpendicular to the x axis at a distance L from the sample position. The real-space coordinate at the center of pixel (i, j) is (L, y_i, z_i) . Each pixel has a width Δy and a height Δz . BornAgain requires a full parametrization of the detector geometry to correctly perform the affine-linear mapping from pixel indices i, j to pixel coordinates x_i, y_i ; see the [rectangular detector tutorial](#).

Since the differential scattering cross section (1.35) is given with respect to a solid-angle element $d\Omega$, we need to express the scattered wavevector \mathbf{k}_f in spherical coordinates, using the horizontal azimuth angle ϕ_f and the vertical glancing angle α_f . The projection of (α_f, ϕ_f) into the detector plane (y, z) is known as the *gnomonic projection*. From elementary trigonometry one finds

$$\begin{aligned} y &= L \tan \phi_f, \\ z &= (L / \cos \phi_f) \tan \alpha_f. \end{aligned} \tag{5.1} \quad \{\text{Eyzdet}\}$$

Fig. 5.2 shows lines of equal α_f, ϕ_f in the detector plane. To emphasize the curvature of the constant- α_f lines, scattering angles up to more than 25° are shown. In typical SAS

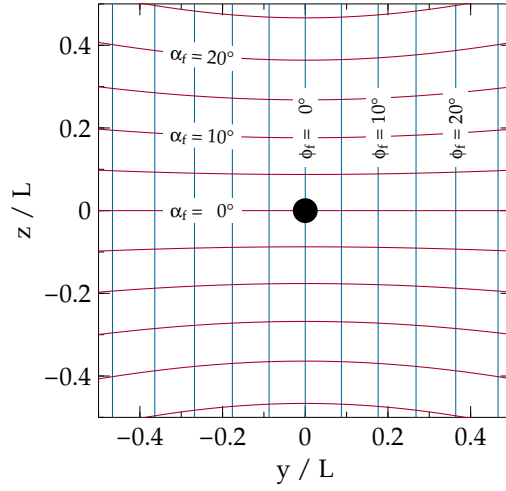


Figure 5.2: Lines of constant α_f (red) or ϕ_f (blue) in the detector plane, for a planar detector at distance L from the sample. The black dot indicates the beamstop location for the central incident beam (SAS geometry, $\hat{\mathbf{k}}_i = \hat{x}$).

`{Fconstalphi}`

or GISAS, scattering angles are much smaller, and therefore the mapping between pixel coordinates and scattering angles is in a good first approximation linear. Of course BornAgain is not restricted to this linear regime, but uses the exact nonlinear mapping (5.1).

To determine the scattering vector \mathbf{q}_{ij} that corresponds to a pixel (i, j) , we need to express the outgoing wavevector \mathbf{k}_f as function of y and z . This can be done either by inverting (5.1) and inserting the so obtained $\alpha_f(y, z)$ and $\phi_f(y)$ in

$$\mathbf{k}_f = K \begin{pmatrix} \cos \alpha_f \cos \phi_f \\ \cos \alpha_f \sin \phi_f \\ \sin \alpha_f \end{pmatrix}, \quad (5.2) \quad \text{\code{{E}kf_by_angle}}$$

or much more directly by using geometric similarity in Cartesian coordinates. The result is rather simple:

$$\mathbf{k}_f = \frac{K}{\sqrt{L^2 + y^2 + z^2}} \begin{pmatrix} L \\ y \\ z \end{pmatrix}. \quad (5.3) \quad \text{\code{{E}kf_by_pixel}}$$

The transform (5.6) between pixel coordinates y, z and physical scattering vector components q_y, q_z is nonlinear, due to the square-root term in the denominator of (5.3). For $y, z \ll L$, however, nonlinear terms loose importance.

The left detector frame in Fig. 5.3 shows circles of constant values of $\pm q_x$. For given steps in q_x , the distance between adjacent circles increases towards the detector center. From ?? and (5.3), one finds asymptotically for $y, z \rightarrow L$ that q_x goes with the

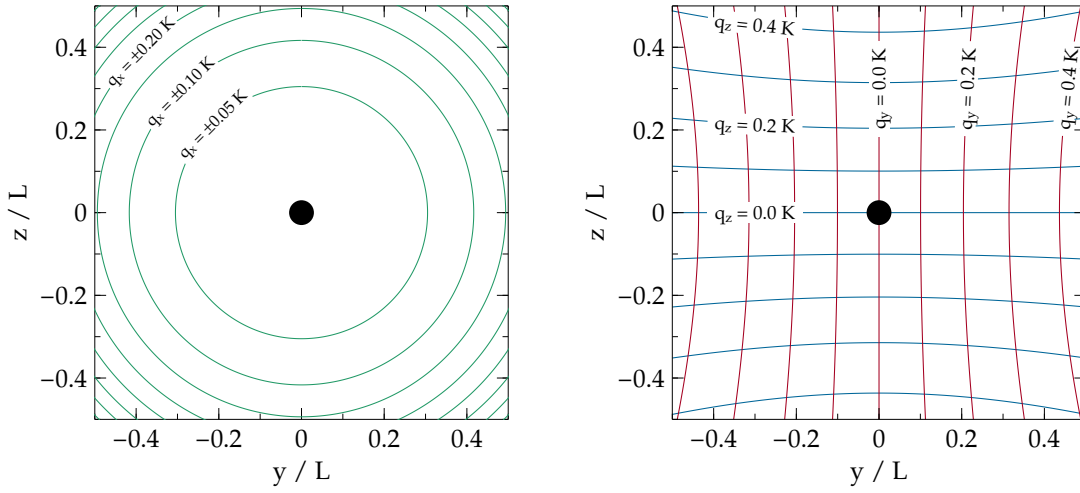


Figure 5.3: Lines of constant q_x (left), q_y or q_z (right), in units of the incident wavenumber $K = 2\pi/\lambda$, for a planar detector. SAS geometry as in Fig. 5.2.

{Fconstq}

square of the two other components of the scattering vector,

$$\frac{q_x}{K} \doteq \frac{y^2 + z^2}{2L^2} \doteq \frac{q_y^2 + q_z^2}{2K^2}. \quad (5.4) \quad \{\{Eqxasy\}\}$$

Therefore, under typical small angle conditions $y, z \rightarrow L$ the dependence of the scattering signal on q_x is unimportant: one basically measures $v(\mathbf{q}) \simeq v(0, q_y, q_z)$. The exception, for sample structures with long correlations in x direction, is illustrated in Fig. 5.4.

As anticipated in (5.4), the other two components of \mathbf{q} are in first order linear in the pixel coordinates,

$$\frac{q_y}{K} = \frac{y}{L} \left(1 - \frac{y^2 + z^2}{2L^2} + \dots \right), \quad (5.5) \quad \{\{Eqxasy\}\}$$

and similarly for q_z . The nonlinear correction terms lead to the pincushion distortion shown in the right detector frame in Fig. 5.3.

Since pixel coordinates are meaningful only with respect to a specific experimental setup, users may wish to transform detector images towards the physical coordinates q_y and q_z . As shown in Fig. 5.5, this would yield a barrel-shaped illuminated area in the q_y, q_z plane.

To summarize this section, the wavevector \mathbf{q}_{ij} can be determined from the pixel

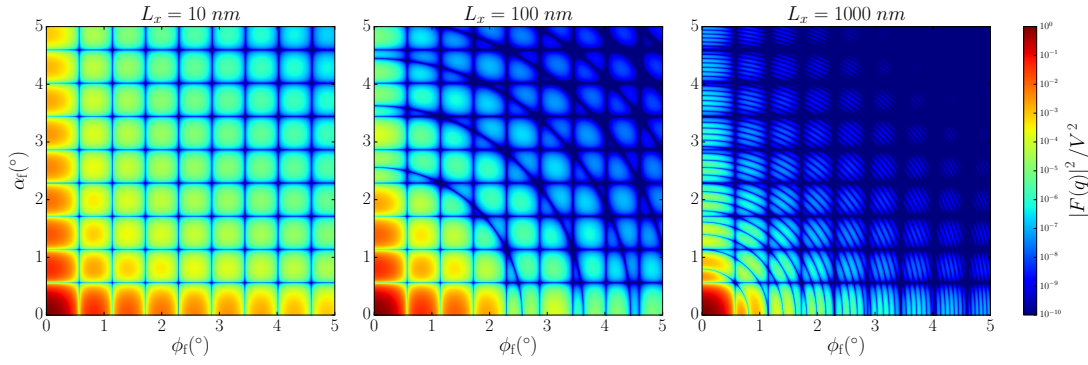


Figure 5.4: Simulated detector image for small-angle scattering from uncorrelated cuboids (right rectangular prisms). The incoming wavelength is 0.1 nm. The prisms have edge lengths $L_y = L_z = 10$ nm; the length L_x , in beam direction, is varied as shown above the plots. The circular modulation comes from a factor $\text{sinc}(q_x L_x/2)$ in the cuboid form factor, with q_x given by (5.4).

{Fdetbox}

indices through the following steps:

$$\begin{aligned}
 &(i, j) \\
 &\quad \downarrow \quad \text{calibrate of origin, then employ affine-linear mapping} \\
 &(y, z) \\
 &\quad \downarrow \quad \text{use (5.3)} \\
 &\mathbf{k}_f \\
 &\quad \downarrow \quad \text{use (??)} \\
 &\mathbf{q}
 \end{aligned} \tag{5.6} \quad \{\{\text{Eqalgo}\}\}$$

Transforming detector images from pixel coordinates into the q_y, q_z plane is not implemented in BornAgain, and not on our agenda. We would, however, like to hear about use cases.

When simulating and fitting experimental data with BornAgain, detector images remain unchanged. All work is done in terms of reduced pixel coordinates y/L and z/L . Corrections are applied to the simulated, not to the measured data.

...show how to plot q grid on top of detector image ...

5.2.2 Intensity transformation

The solid angle under which a detector pixel is illuminated from the sample is in linear approximation

$$\Delta\Omega = \cos\alpha_f \Delta\alpha_f \Delta\phi_f = \cos\alpha_f \left| \frac{\partial(\alpha_f, \phi_f)}{\partial(y, z)} \right| \Delta y \Delta z = \cos^3\alpha_f \cos^3\phi_f \frac{\Delta y \Delta z}{L^2}. \tag{5.7} \quad \{\{\text{Eqalgo}\}\}$$

Altogether, the expected count rate in detector pixel (i, j) is proportional to

$$I_{ij} = \cos^3\alpha_f \cos^3\phi_f \frac{d\sigma}{d\Omega}(\mathbf{q}_{ij}), \tag{5.8} \quad \{\{\text{Eitrafo_cos}\}\}$$

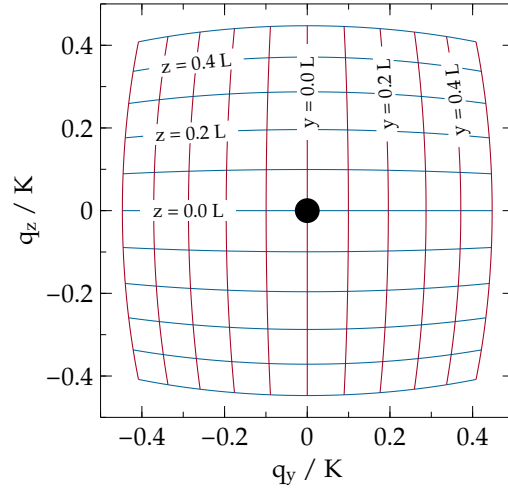


Figure 5.5: The outer contour of the blue and red grid shows the border of a square detector image after transformation into the physical coordinates q_y , q_z . The blue and red curves correspond to horizontal and vertical lines in the detector.

{Fconstp}

where we have omitted constant factors L^{-2} , Δy and Δz . Using pixel coordinates instead of angles, this can be rewritten as

$$I_{ij} = \left(1 + \frac{y^2 + z^2}{L^2}\right)^{-3/2} \frac{d\sigma}{d\Omega}(\mathbf{q}_{ij}(y, z)). \quad (5.9) \quad \{\{E\text{Itrafo_pix}\}\}$$

Bibliography

- [1] G. Pospelov, W. Van Herck, J. Burle, J. M. Carmona Loaiza, C. Durniak, J. M. Fisher, M. Ganeva, D. Yurov and J. Wuttke, *J. Appl. Cryst.* **53**, 262 (2020). ii, 1:1, 1:5, 3:11
- [2] V. P. Sears, *Neutron News* **3**, 26 (1992). 1:2
- [3] V. P. Sears, *Neutron Optics*, Oxford University Press: Oxford (1989). 1:2
- [4] F. Mezei, *Physica B+C* **137**, 295 (1986). 1:3
- [5] C. F. Majkrzak, K. V. O'Donovan and N. F. Berk, in *Neutron Scattering from Magnetic Materials*, edited by T. Chatterji, Elsevier: Amsterdam (2006). 1:3, 4:21
- [6] G. Renaud, R. Lazzari and F. Leroy, *Surf. Sci. Rep.* **64**, 255 (2009). 1:3
- [7] M. v. Laue, *Erg. exakt Naturwiss.* **10**, 133 (1931). 1:4
- [8] G. H. Vineyard, *Phys. Rev. B* **26**, 4146 (1982). 1:6
- [9] P. Mazur and D. L. Mills, *Phys. Rev. B* **26**, 5175 (1982). 1:6
- [10] S. Dietrich and H. Wagner, *Z. Phys. B* **56**, 207 (1984). 1:6
- [11] S. Dietrich and H. Wagner, *Z. Phys. B* **59**, 35 (1985). 1:6
- [12] H. Schober, *J. Neutron Res.* **17**, 109 (2014). 1:7
- [13] J. D. Jackson, *Classical Electrodynamics*, John Wiley: New York (²1975). 2:5
- [14] F. Abelès, *J. Phys. Radium* **11**, 307 (1950). 2:7
- [15] G. Kohn, V, *J. Moscow Phys. Soc.* **1**, 425 (1991). 2:9, 4:9
- [16] S. A. Stepanov, E. A. Kondrashkina, R. Köhler, D. V. Novikov, G. Materlik and S. M. Durbin, *Phys. Rev. B* **57**, 4829 (1998). 2:9, 2:10, 4:9, 4:10
- [17] L. G. Parratt, *Phys. Rev.* **95**, 359 (1954). 2:10
- [18] J. Lekner, *Theory of Reflection*, Springer: Cham (²2016). 3:1, 3:2
- [19] L. D. Landau and E. M. Lifschitz, *Lehrbuch der theoretischen Physik, III. Quantenmechanik*, Akademie-Verlag: Berlin (⁷1985). 3:1, 4:7

- [20] A. V. Andreev, A. G. Michette and A. Renwick, J. Mod. Opt. **35**, 1667 (1988). 3:2
- [21] M. Tolan, *X-ray scattering from soft-matter thin films. Materials science and basic research* (Springer Tracts in Modern Physics 148), Springer: Berlin (1999). 3:3, 3:15
- [22] D. K. G. de Boer and A. J. G. Leenaers, Physica B **221**, 18 (1996). 3:3, 3:14
- [23] L. Névot, B. Pardo and J. Corno, Rev. Phys. Appl. **23**, 1675 (1988). 3:3
- [24] A. Gibaud and G. Vignaud, in *X-ray and Neutron Reflectivity*, edited by J. Dailant and A. Gibaud (Lect. Notes Phys. 770) (2009). 3:3
- [25] S. K. Sinha, E. B. Sirota, S. Garoff and H. B. Stanley, Phys. Rev. B **38**, 2297 (1988). 3:5, 3:10, 3:12, 3:13, 3:15
- [26] V. Holý, J. Kubena, I. Ohlídal, K. Lischka and W. Plotz, Phys. Rev. B **47**, 15896 (1993). 3:5, 3:10, 3:13
- [27] E. W. Weisstein, *Bivariate Normal Distribution*. <https://mathworld.wolfram.com/BivariateNormalDistribution.html>. 3:9
- [28] B. Pynn, Phys. Rev. B **45**, 602 (1992). 3:10, 3:13
- [29] L. Névot and P. Croce, Rev. Phys. Appl. **15**, 761 (1980). 3:10, 3:11, 3:13
- [30] M. Abramowitz and I. Stegun, *Handbook of Mathematical Functions*, National Bureau of Standards (1964). 3:11
- [31] J.-P. Schlomka, M. Tolan, L. Schwalowsky, O. H. Seeck, J. Stettner and W. Press, Phys. Rev. B **51**, 2311 (1995). 3:11, 3:12
- [32] A. Steyerl, Z. Phys. **254**, 169 (1972). 3:13
- [33] Y. A. Baloshin and A. V. Kostin, Optics Commun. **160**, 22 (1999). 3:13
- [34] A. Steyerl, S. S. Malik and L. R. Iyengar, Physica B **173**, 47 (1991). 3:13
- [35] P. Beckmann and A. Spizzichino, *The Scattering of Electromagnetic Waves from Rough Surfaces*, Artech House: Norwood, MA (1987). 3:13
- [36] V. Holý and T. Baumbach, Phys. Rev. B **49**, 10668 (1994). 3:14
- [37] U. Pietsch, V. Holý and T. Baumbach, *High-Resolution X-Ray Scattering*, Springer: New York (2004). 3:14
- [38] D. K. G. de Boer, Phys. Rev. B **49**, 5817 (1994). 3:14, 3:15, 3:16
- [39] D. K. G. de Boer, Phys. Rev. B **53**, 6048 (1996). 3:14, 3:15, 3:16
- [40] D. K. G. de Boer, Phys. Rev. B **44**, 498 (1991). 3:14

- [41] D. K. G. de Boer, Phys. Rev. B **51**, 5297 (1995). 3:14, 3:15
- [42] A. Caticha, Phys. Rev. B **52**, 9214 (1995). 3:15
- [43] M. Rauscher, T. Salditt and H. Spohn, Phys. Rev. B **52**, 16855 (1995). 3:15
- [44] S. Dietrich and A. Haase, Phys. Rev. **260**, 1 (1995). 3:15
- [45] H. Ogura and N. Takahashi, Progress in Electromagnetic Research PIER **14**, 89 (1996). 3:15
- [46] B. P. Toperverg, O. Schärpf and I. S. Anderson, Physica B **276–278**, 954 (2000). 3:15
- [47] Y. Fujii, IOP Conf. Series: Mat. Sci. and Eng. **42**, 012009 (2011). 3:15
- [48] Y. Fujii, Acta Cryst. A **56** (2013). 3:15
- [49] Y. Fujii, Japan. J. Appl. Phys. **53**, 05FH06 (2014). 3:15
- [50] Y. Fujii, T. MRS Jap. **40**, 369 (2015). 3:15
- [51] F. N. Chukhovskii, Acta Cryst. A **67**, 200 (2011). 3:16
- [52] F. N. Chukhovskii, Acta Cryst. A **68**, 505 (2012). 3:16
- [53] F. N. Chukhovskii and B. S. Roshchin, Acta Cryst. A **71**, 612 (2015). 3:16
- [54] R. Maruyama, D. Yamazaki and K. Soyama, J. Phys. Soc. Jpn. **22** (2018). 3:16
- [55] A. Hafner, PhD thesis, University Libre de Bruxelles, Institutue Laue-Langevin (2019). 3:16
- [56] E. Kentzinger, U. Rücker, B. Toperverg, F. Ott and T. Brückel, Phys. Rev. B **77**, 104435 (2008). 4:4, 4:11, 4:15
- [57] E. Kentzinger, U. Rücker and B. Toperverg, Physica B **335**, 82 (2003). 4:4, 4:6, 4:11, 4:15
- [58] B. P. Toperverg, Phys. Met. Metallogr. **116**, 1337 (2015). 4:12
- [59] A. R. Wildes, Review of Scientific Instruments **70**, 4241 (1999). 4:13
- [60] A. R. Wildes, Neutron News **17**, 17 (2006). 4:13

List of Symbols

\perp	Normal to the xy sample plane, 2:1
\parallel	Parallel to the xy sample plane, 2:1
\pm	Upward (+) or downward (−) propagating, 2:2
β	Imaginary part of the refractive index, 1:7
$\delta v_l(\mathbf{q})$	Fourier transform of the SLD $\delta v(\mathbf{r})$, evaluated in one sample layer, 2:5
δ	Small parameter in the refractive index $n = 1 - \delta + i\beta$, 1:7
ϵ_0	Vacuum permittivity, 8.854...As/Vm, 1:3
$\epsilon(\mathbf{r})$	Relative dielectric permittivity function, 1:4
$\epsilon(\mathbf{r})$	Relative dielectric permittivity tensor, 1:3
$\bar{v}(\mathbf{r})$	Distortion field, 1:6
μ_0	Vacuum permeability, $4\pi \cdot 10^{-7}$ Vs/Am, 1:3
μ_n	Magnetic moment of the neutron, 1:3
$\mu(\mathbf{r})$	Relative magnetic permeability tensor, 1:3
$\hat{\rho}$	Density matrix operator, 1:2
$\rho(\mathbf{r})$	Electron number density, 1:4
ρ_s	Number density of chemical element s , 1:2
σ	Scattering or absorption cross section, 1:7
$\boldsymbol{\sigma}$	Pauli vector, composed of the three Pauli matrices: $\boldsymbol{\sigma} = (\sigma_x, \sigma_y, \sigma_z)$, 1:3
$\phi(z)$	z -dependent factor of $\psi(\mathbf{r})$, 2:2
$\chi_l(z)$	Indicates whether z is in layer l , 2:4
$\psi(\mathbf{r})$	Stationary wavefunction, 1:1
$\psi(\mathbf{r}, t)$	Microscopic neutron wavefunction, 1:1

$\psi^\pm(\mathbf{r})$	Upward (+) or downward (−) propagating component of $\psi(\mathbf{r})$, 2:2
$\Psi(\mathbf{r})$	Generic wave amplitude, possibly vectorial or spinorial, 1:5
$\Psi(\mathbf{r})$	Stationary coherent spinor wavefunction, 1:3
ω	Frequency of incident radiation, 1:1
Ω	Solid angle, 1:7
A_{wl}^\pm	Amplitude of the plane wave $\phi_{wl}^\pm(\mathbf{r})$, 2:4
b	Bound scattering length, 1:2
$\mathbf{B}(\mathbf{r}, t)$	Magnetic field, 1:3
c. c.	Complex conjugate, 1:4
$D_0(\mathbf{r})$	Differential operator in the vacuum wave equation, 1:5
$D(\mathbf{r})$	Differential operator in the wave equation, 1:6
$\mathbf{D}(\mathbf{r}, t)$	Displacement field, 1:3
$\mathbf{E}(\mathbf{r}, t)$	Electric field, 1:3
$\mathbf{b}(\mathbf{r})$	Rescaled field $\mathbf{b} = (m\mu/2\pi\hbar^2)\mathbf{B}$, 1:3
$\mathbf{B}(\mathbf{r}, t)$	Magnetic induction, 1:3
$\mathbf{J}(\mathbf{r})$	Flux, 1:2
k_\perp	Component of \mathbf{k} along the sample normal, 2:1
k_l	Wavenumber in layer l , 2:3
\mathbf{k}	Wave vector, 1:2
\mathbf{k}_\parallel	Projection of \mathbf{k} onto the sample plane, 2:1
K	Wavenumber in vacuum, 1:1
l	Layer index, 2:3
n_l	Refractive index of layer l , 2:3
n	Refractive index, 1:6
\mathbf{n}	Normal vector of an interface, 2:5
N	A multilayer sample has N layers, including the semi-infinite bottom and top layers, 2:4
p_j	Probability of state j , 1:2

r_e	Classical electron radius $2.817 \dots^{-15}$ m, 1:4
\mathbf{r}	Position, 1:1
\mathbf{S}	Poyinting vector, 1:4
t	Time, 1:1
$\delta\hat{v}(\mathbf{r})$	Perturbation potential, 1:6
$v_{\text{nucl}}(\mathbf{r})$	Rescaled neutron potential, scattering length density (SLD), 1:2
$V(\mathbf{r})$	Neutron potential, 1:1
$\hat{v}(\mathbf{r})$	Generic potential, 1:5
x	Horizontal coordinate, in the sample plane, 2:1
y	Horizontal coordinate, in the sample plane, 2:1
z_l	Vertical coordinate at the top of layer l (at the bottom for $l = 0$), 2:4
z	Vertical coordinate, along the sample normal, 2:1

Index

- Abelès matrix, 2:7
- Absorption, 1:7
- Atomic scale, 1:2

- B* Field, *see* Magnetic field
- BA, *see* Born approximation
- Background
 - diffuse, 1:2
- Backtracking, 2:2
- Born approximation, 1:6, 1:7
 - elastic scattering cross section, 1:7
- Bound scattering length, *see* Scattering length
- Box (form factor), 5:5
- Bragg scattering, 1:2

- Circular modulation, 5:5
- Classical electron radius, 1:4
- Coherent scattering length, 1:2
- Convention
 - coordinate system, 5:2
 - horizontal plane, 2:1
 - interface coordinate, 2:3, 2:4
 - layer numbering, 2:3, 2:4
 - p- and s-polarization, 2:5, 2:6
 - sign convention, 1:3
 - vertical direction, 2:1
- Coordinate
 - interface, 2:3, 2:4
- Coordinate system, 5:2
- Correlation
 - atomic scale, 1:2
- Cross section, 1:2, 1:7
 - Born approximation, 1:7
- Crystallographic sign convention, 1:3
- Cuboid (form factor), 5:5
- Current density, *see* Flux

- Damping, 1:3
 - inelastic scattering, 1:1
- Density, 1:2
 - electron, 1:4
- Density matrix, 1:2
- Detector
 - background, 1:2
 - backtracking, 2:2
 - calibration, 5:2
 - distortion of q_x , q_y grid, 5:4
 - illumination angle correction factor, 5:5
 - pixel coordinate, 5:2
 - transmission geometry, 2:9
- Dielectric permittivity, 1:4
- Dispersion
 - X-ray, 1:4
- Dispersion relation
 - neutron, 1:1
- Distorted wave, 1:6
 - operator, 1:6
 - wave equation, 1:6
- Distorted-wave Born approximation, 1:6, 1:7
 - multilayer, 2:4
- Distortion
 - of q_x , q_y grid in detector plane, 5:4
- Distortion field, 1:6

- Elastic scattering, *see also* Cross section, 1:3
- Electric field, 1:3
- Electron density, 1:4
- Electron radius, 1:4
- Exciting wave
 - DWBA, 2:1

- Fermi's pseudopotential, 1:2
- Field
 - magnetic, *see* Magnetic field
- Flux
 - incident and scattered, 1:7
 - neutron, 1:2
 - reflected, 2:2

- transmitted, 2:2
- X-rays, 1:4
- FormFactorBox, 5:5
- Fresnel coefficients, 2:3, 2:6
- GISAS, *see* Grazing-incidence small-angle scattering
- Glancing angle, 2:1
- Gnomonic projection, 5:2
- Grazing incidence, 1:7
- Grazing-incidence small-angle scattering, 1:1, 1:6
 - dielectric model, 1:4
- H Field, *see* Magnetizing field
- Horizontal plane, 2:1
- Horizontal wavevector, 2:2
- Illumination
 - detector, 5:5
- Incident radiation
 - flux, 1:7
- Incoherent scattering, 1:2
- Index of refraction, *see* Refractive index
- Indicator function, 2:4
- Inelastic scattering, 1:1, 1:2
- Instrument, 5:1
- Interface
 - coordinate, 2:3, 2:4
- Isotope, 1:2
- Laue model, 1:4
- Layer
 - index, 2:3, 2:4
 - refractive index profiles, 2:3
 - transfer matrix, 2:7
- Layered structure, *see* Multilayer
- Loss terms, *see* Damping
- Magnetic field, 1:3
 - neutron propagation, 1:3
- Magnetic moment
 - neutron, 1:3
- Magnetic permeability, 1:3, 1:4
- Magnetizing field, 1:3
 - coupling to neutron moment, 1:3
 - reduced, 1:3
- Mapping
 - wavevector to pixel coordinate, 5:2
- Maxwell's equations, 1:3
- Mixed quantum state, 1:2
- Monochromatic wave, 1:1, 1:3

- Multilayer, 2:1–2:14
 - coordinates, 2:3, 2:4
 - numbering, 2:3, 2:4
 - refractive index profiles, 2:3
 - transfer matrix, 2:7
- Multiple reflections, 2:3
- Neutron
 - dispersion relation, 1:1
 - magnetic moment, 1:3
 - optical potential, 1:2
 - optics, 1:2
 - polarized, 4:1
 - potential, 1:1, 1:2
 - spin, 1:2–1:3
 - wave propagation, 1:1–1:3
- Normalization
 - neutron wavefunction, 1:2
- Number density, 1:2, *see* Density
- Numbering
 - layers, 2:3, 2:4
- Optics
 - neutron, 1:2
- p -Polarization, 2:5, 2:6
- Pauli matrix, 1:3
- Pauli vector, 1:3
- Permeability, 1:3, 1:4
- Permittivity, 1:4
- Perturbation potential, 1:6
- Phase factor, 1:1, 1:3
- Pincushion distortion, 5:4
- Pixel, *see* Detector
- Plane
 - wave, 1:6
- Plane wave, 1:2
- Polarization, 1:3
 - neutron, 4:1
 - p and s , 2:5, 2:6
- Potential
 - generic, 1:5
 - neutron, 1:1, 1:2
 - optical, 1:2
 - perturbation, 1:6
- Poynting vector, 1:4
- Prism (form factor)
 - rectangular (Box), 5:5
- Projection
 - wavevector to pixel coordinate, 5:2
- Pseudopotential
 - Fermi's, 1:2

- Pure quantum state, 1:2
- Quantum state
 - pure vs mixed, 1:2
- Quantum-mechanical convention, 1:3
- Reflectance, 2:2
- Reflection, 1:7, 2:1, *see also* Fresnel
 - coefficients
 - coefficient, 2:2
 - multiple, 2:3
- Reflectometer
 - vertical vs horizontal, 2:1
- Refraction, 1:7, 2:1
 - Snell's law, 2:4
- Refractive index, 1:6
 - losses from Bragg scattering, 1:2
 - losses from incoherent scattering, 1:2
 - losses from inelastic scattering, 1:1
 - profile, 1:7
 - sign convention, 1:7
 - vertical variation, 2:1
- s*-Polarization, 2:5, 2:6
- Sample normal, 2:1
- Sample plane, 2:1
- SAS, *see* Small-angle scattering
- Scattered radiation
 - backtracking, 2:2
- Scattering
 - Bragg, 1:2
 - cross section, 1:2, 1:7
 - diffuse, 1:2
 - elastic, 1:1, 1:3
 - geometry, 1:7
 - grazing incidence, *see*
 - Grazing-incidence small-angle scattering
 - incoherent, 1:2
 - inelastic, 1:1, 1:2
 - matrix, 1:7
 - small-angle, 1:2
- Scattering length, 1:2
 - coherent, 1:2
- Scattering length density, 1:2
- Schrödinger equation
 - macroscopic, 1:3
 - microscopic, 1:1
- Sign convention
 - refractive index, 1:7
 - wave propagation, 1:3
- SLD, *see* Scattering length density
- Small-angle scattering, 1:2, 1:8
 - dielectric model, 1:4
- Snell's law, 2:4
- Spin, 1:3
 - neutron, 1:2
- Spinor, 1:3
- Stationary wavefunction, 1:1
- Time dependence
 - dielectric permittivity, 1:3
 - neutron potential, 1:1
- Transfer matrix, 2:7
- Transformation
 - wavevector to pixel coordinate, 5:2
- Transition matrix, *see* Scattering matrix
- Transmission, *see* Fresnel coefficients
- Transmission geometry, 2:9
- Transmittance, 2:2
- Unit
 - neutron wavefunction, 1:2
- Unperturbed distorted wave equation, 1:6
- Vacuum, 1:6
 - neutron wavenumber, 1:1
 - wave operator, 1:5
- Vertical direction, 2:1
- Vertical wavenumber, 2:2
- Wave
 - distorted, 1:6
 - exciting, 2:1
 - monochromatic, 1:1, 1:3
 - operator
 - distorted, 1:6
 - vacuum, 1:5
 - plane, 1:2, 1:6
- Wave equation
 - generic, 1:5
 - unperturbed distorted, 1:6
 - X-ray, 1:4
- Wave propagation, *see also* Sign
 - convention, 1:1–1:3
 - in multilayer, 2:1–2:2
 - neutron, 1:1–1:3
 - X-ray, 1:3–1:4
- Wavenumber
 - neutron, 1:1
 - vertical, 2:2
- Wavevector
 - complex, 2:4
 - horizontal, 2:2

X-ray

flux, 1:4

scattering theory, 1:8

wave equation, 1:4

wave propagation, 1:3–1:4